

1960

Web buckling tests on welded plate girders. Part 4: tests on plate girders subjected to combined bending and shear. WRC Bulletin, 64, (September 1960), Reprint No. 165 (60-5)

K. Basler

J. A. Mueller

B. Thurlimann

B. T. Yen

Follow this and additional works at: <http://preserve.lehigh.edu/engr-civil-environmental-fritz-lab-reports>

Recommended Citation

Basler, K.; Mueller, J. A.; Thurlimann, B.; and Yen, B. T., "Web buckling tests on welded plate girders. Part 4: tests on plate girders subjected to combined bending and shear. WRC Bulletin, 64, (September 1960), Reprint No. 165 (60-5)" (1960). *Fritz Laboratory Reports*. Paper 67.

<http://preserve.lehigh.edu/engr-civil-environmental-fritz-lab-reports/67>

This Technical Report is brought to you for free and open access by the Civil and Environmental Engineering at Lehigh Preserve. It has been accepted for inclusion in Fritz Laboratory Reports by an authorized administrator of Lehigh Preserve. For more information, please contact preserve@lehigh.edu.

251.14

LEHIGH UNIVERSITY LIBRARIES



3 9151 00897580 3

INDEXED



251.14

LEHIGH UNIVERSITY INSTITUTE OF RESEARCH

WELDED PLATE GIRDERS

REPORT NO. 251-14

WEB BUCKLING TESTS ON WELDED PLATE GIRDERS

PART 4: TESTS ON PLATE GIRDERS SUBJECTED TO COMBINED BENDING AND SHEAR

KONRAD BASLER
BUNG-TSENG YEN
JOHN A. MUELLER
BRUNO THÜRLIMANN

3 copies
no. 2

Welded Plate Girders, Report No. 251-14

Submitted to the
Welded Plate Girder Project Committee
for approval as a publication

WEB BUCKLING TESTS ON WELDED
PLATE GIRDERS

Part 4: Tests on Plate Girders Subjected to
Combined Bending and Shear

by

Basler, K., Yen. B. T., Mueller, J. A., and Thurlimann, B.

Fritz Engineering Laboratory
Lehigh University
Bethlehem, Pennsylvania
May 1960

FRITZ ENGINEERING LABORATORY
LEHIGH UNIVERSITY
BETHLEHEM, PENNSYLVANIA

FOREWORD

This is the fourth part of a report on plate girder tests conducted at Lehigh University. Reference must be made to the first part, Report No. 251-11, for the scheme of publication, the properties of the girders, the nomenclature, and the list of references.

4.1 Introduction

While the girders discussed in part 2 and part 3 were subjected to pure bending and high shear respectively, those in this test series were studied under the combined action of bending and shear. It is the purpose of this report to explain how the investigation was carried out and what observational facts were obtained.

Each bending girder discussed in part 2 consisted of a middle section, which was the test section proper, and two end pieces which had stronger webs than the test section. Since failure always occurred as intended in the preselected test section, it was possible to splice together the undamaged end pieces and form new girders to be tested to destruction. This was done with the end pieces of girders G1, G2, G4, and G5 and the resulting girders are termed E1, E2, E4, and E5, respectively. If these spliced specimens were tested in the setup sketched in Fig. 1.3, bending failures would almost invariably result because flange yielding would always precede exhaustion of the shear strength of the relatively strong web. Thus, in order to achieve a more severe interaction between bending and shear, these girders had to be modified.

The adaptation decided upon was to weld cover plates to both flanges of the spliced portions. Using different sizes and numbers of cover plates for the group of girders having the same web thickness, girders E1, E4, and E5, the shear to normal stress ratio $\xi = \tau/\sigma$ (Sec. 1.1) was sufficiently adjusted to render a variety of combinations of bending and shear stresses. For E4, cover plates 15" x 7/8" were added such that the girder would fail simultaneously in bending and shear. Girder E1 was assigned one more cover plate than E4 to ensure shear failures, this additional plate being 18" x 3/4". On the other hand, girder E5 had no cover plates.

Having provided a sufficient range of the ratio of shear stress to normal stress to investigate its influence, the effect of the web slenderness ratio was the next thing to be studied. Girders E2, G8, and G9 were designed for this purpose. Using the end pieces of girder G2 with added cover plates of 16" x 1", girder E2 was formed with a one half inch web. G8 and G9, two new girders, had the same span, depth, and fabrication details as the E-girders, but had quite slender webs of three-sixteenths and one-eighth of an inch, resulting in web slenderness ratios of about 254 and 382 respectively.

Thus, this third phase of the investigation consisted of a total of six girders referred to as E1, E2, E4, E5, G8, and G9. For the cross sectional dimensions and constants, material properties, and the girders' reference loads and deflections, the summary tables of Part 1 must be consulted.

4.2 Test Setup

The girders of this series were tested in the 5,000,000 pound Baldwin Universal Testing Machine at Fritz Engineering Laboratory. With the movable crosshead of the machines guided by massive columns, the movement is strictly vertical without horizontal or torsional displacements. For this reason, all girders were mounted on rollers at both supports. Although they had one degree of freedom while resting in the test bed, the girders became stable as soon as the load was applied. This system is illustrated in Fig. 1.3.

In the design of the girders subjected to bending or shear, a predetermined test section could be designed. In this series of girders subjected to combined bending and shear, the test setup precludes any such section and failure can occur anywhere. The entire girder is the test section proper. If failure should occur under the point of load application, it would be difficult to trace its primary cause. While this is a disadvantage from the

research point of view, these tests simulate true field conditions. The setup used, when inverted, reproduces the conditions at an intermediate support of a continuous girder where the ends of the test girder are at the points of inflection.

Appearing in Fig. 4.1 is the test setup, where a girder is seen positioned in the testing machine. Besides the elevation, a plan view of the girder is provided which shows the lateral bracing system. Incorporated in this system were the supports, the loading point, and two lateral bracing pipes. While the friction forces at the loading surface fixed the girder against any lateral buckling at its midspan, the support points under load eliminated lateral movements in their vicinity. The two lateral braces were located at quarter points with their far ends attached to a rigid bracing beam. The connecting pins at both ends of each bracing pipe were fitted snug in the holes so that, unlike the setup for the bending girders, no lateral movement of girder was allowed before the braces acted.

Of importance in the subsequent presentation of results is the orientation of a girder. To this end, the Cartesian coordinate system shown in Fig. 1.3 is needed. All drawings containing a girder's or panel's outline will be presented such that the x-axis points to the right, that is, the lateral braces are hidden behind the girder.

4.3 Test Results

In this section the tests conducted on the six girders are explained and the results of all basic observations presented. Among the "basic" measurements made throughout the investigation are the centerline deflection, the state of strain at a panel's center, the extension of a panel's diagonals, the strains in a transverse stiffener, and the web deflection at the centers of certain panels. Since the method of presentation is substantially the same for all specimens, the data will be thoroughly explained for girder E1 only.

For a survey of properties of girder E1, Table 1.1 in part 1 of this report should be consulted. There it is shown that the web depth to web thickness ratio was $\beta = 131$, and that a total of four tests were run which produced failure in panels of aspect ratios $\alpha = 3.0, 1.5, 1.5,$ and 1.0 .

The load-deflection curve, Fig. 4.2, together with the sketches shown in Fig. 4.3, completely describe the testing history of girder E1. From these figures it is seen that the specimen was loaded up to load No. 7 at 540 kips in its first loading cycle. After reducing to zero, this load was alternately reapplied and reduced to near zero ten times without causing any additional deflections.

It is seen that when the applied load was increased above load No. 7, the highest load which could be statically maintained, the ultimate load, was 555 kips. Upon unloading to load No. 15, the first test was complete. In this test a clear shear failure occurred in the long panel where $\alpha = 3.0$, as is indicated by the right hand sketch in the first row of Fig. 4.3. A photograph of the failed panel is included as Fig. 4.4 where it can be seen that permanent web distortion was located along the general direction of the yield lines. However, this distortion was small enough that the panel could be reinforced by two pairs of transverse stiffeners fitted to the distorted shape and welded to the web at its third points, as seen in the third sketch of Fig. 4.3. This reinforcing operation is always indicated by a welding symbol in the load-deflection diagrams.

The second test, T2, extended from load No. 16 to load No. 24. According to the definition adopted in Sec. 2.4, the ultimate load for this test was attained at load No. 22, where $P_u = 580$ kips. Occurring in the panel to the right of the loading point, this failure was identified as a shear failure, as the photograph of Fig. 4.5 reveals. Fig. 4.6 is a photograph taken of the far side of this failed panel. Evidently, the width of the yielded strip as appearing in these pictures must not be identified

with the effective width of a tension field, since they only reveal surface conditions. As pointed out before, Fig. 3.12, the stresses at the surface are due to both plate membrane and bending stresses, whereas the tension field is entirely a membrane action.

After completion of the second test, the failed panel was reinforced by welding two single, half inch thick stiffeners to the far side of the web, Fig. 4.3, third sketch on the left. Upon loading again in test T₃, the recorded centerline deflections followed the predicted ones fairly well up until load No. 29. It is interesting to observe that the load-deflection curve exhibited a type of hysteresis loop. This was due to the fact that before being reinforced, the panels acting in a tension field manner underwent greater shear deformations than those predicted by simple beam action. However, after adding rigid and closely spaced transverse stiffeners, the shear force in this panel was essentially carried by beam action and the predicted deflections were followed more closely.

Following the load-deflection curve again, the load was increased to 568 kips and then dropped back to load No. 31, 542 kips, which was less than the P_u obtained from

T2. Since calculations indicated a load well in excess of the ultimate load of T2, this action was unexpected. Upon investigation, it was found to be due to failure of a reinforcing stiffener at $X = -109$. This stiffener, welded with the one on the opposite side of the web as a reinforcement after test T1 to form a 8" x 1/4" plate, did not act similar to the original stiffeners of exactly the same size. The web distortion remaining from the previous test affected the stiffener, which acted as a post, and caused the failure. The repair of this local failure was accomplished by welding a strong compression diagonal in the end panel, as seen from the fourth sketch on the left of Fig. 4.3. Then, the buckled stiffener, relieved of its post action, endured any further increases in the web deflections throughout the following tests.

This diagonal reinforcement, added between load No. 32 and load No. 33, is again indicated in Fig. 4.2 by a welding symbol. Continuing with T3, an ultimate load of $P_u = 634$ kips was reached at load No. 39 and an unloading curve furnished by loads No. 40 and 41. Again, failure was in a shear pattern which occurred in the end panel extending from $X = +84$ to $X = +159$. The corresponding sketch in Fig. 4.3 shows the additional yield lines created by this third test, while Fig. 4.7 gives a photographic verification of this failure.

Having produced a shear failure in each panel of the original girder, the testing could be regarded as finished. However, to satisfy curiosity as to how strong the newly formed square panels on the left side were, the right end panel was reinforced and a fourth test performed. Although subjected to great initial distortions, these square panels were strong enough to allow an increase in the ultimate load of 50 kips, with $P_u = 684$ kips, and held through quite an amount of straining. Although no unloading had taken place due to this straining, the testing of girder E1 was ended with load No. 53.

In order to distinguish the tests conducted on panels which failed in a previous ultimate load test from original tests, the letter r, referring to retesting, is added to their ultimate loads listed in Table 4.1. Since the reinforcing stiffeners were cut to the shape of the distorted web, the panel borders were not in a plane. Therefore, the test results should not be used other than to show that under unfavorable circumstances certain loads could still be carried.

Attention is now focused to Fig. 4.8, a diagram which compares the actual state of stress in the web to that predicted by beam theory. The comparison appears at the very location on the girder where the strain rosette

measurements were taken. The loads Nos. 17, 18, 19, and 20 were selected as representative ones for this study. The choice was influenced by the desire to have these measurements made within the range of a previous loading cycle (Sec. 3.4), and preferably in the particular test where failure occurred in the instrumented panel.

All principal stresses were determined in the same manner described in Sec. 3.4, where the solid stress vectors are the experimental results and the dotted ones computed according to the beam theory. Again, the comparison between experimental and theoretical stresses shows that, even in girders with relatively sturdy webs, a tension field action occurs.

The above conclusion is also confirmed by strain measurements recorded on the pair of intermediate stiffeners bordering the failed panel. In Fig. 4.9 is a curve of applied load versus stiffener strain as observed throughout the second test on this girder. The resulting strain, plotted as abscissa, is the average of four SR-4 gages. Since the stiffeners used throughout the entire investigation were the same, the same layout of gages was used as for girders G6 and G7. For a proper interpretation of this group of measurements, reference should be made to Sec. 3.4.

Another basic observation consistently made was the measurement of the change in distance between two points at the ends of the panel's diagonals. With gage marks drilled in girder panels' corners, the changes in the diagonals were obtained with gages which were similar to Whittemore gage and specially adapted for different panel lengths. All readings were made in the same way as described in Sec. 3.5. As an example, Fig. 4.10 is included showing the movements obtained in T1 and T2, both observed in the same panel shown in Fig. 4.3 where the gage points for these measurements are also shown. The distance between the points in the upper left and lower right was shortened (negative in sign) since this is a "compression diagonal". The other diagonal was stretched. Using a common load ordinate, P, the shortening and extension of the diagonals can be plotted on the same graph and Fig. 4.10 results.

Finally, in Fig. 4.11 some web deflection readings as evaluated and discussed in Sec. 2.3 are presented. As before, the upper half of the figure gives the distorted shapes of the cross sections for a limited number of loads, while the graphs at the bottom give complete load-deflection curves for selected points in the web. A cross section of particular interest is that where the strain rosettes were mounted, at $X = +46 \frac{1}{2}$. From the cross sectional shape

and the graph for this cross section, it is clearly seen that the first test had a pronounced effect on this panel such that the "initial deflections" for the second test, which started with load No. 16, were more than one-half an inch. For the cross section at $X = +121 \frac{1}{2}$, it can be seen that the web was still quite plane at load No. 33, just prior to the test which caused failure in this panel.

With this rather complete explanation of the testing history, the failure modes, and the content of the basic graphs of girder E1, it is possible to study the performance of all the other girders without much further commentary. Therefore, all pertinent graphs and photographs are grouped together at the back of the report for the remaining girders.

In order to study any one girder, the following procedure is suggested:

1. Referring to Table 1.1, obtain the properties of the girder, the number of tests conducted, and the locations of the failures.

2. Use the load-deflection curve to become familiar with the girder's testing history. The curves for girders E2 through G9 are given in Figs. 4.12, 4.22, 4.32, 4.40, and 4.50 respectively. Since the observations were recorded with an Engineer's level, all support movements

were readily eliminated using the principles explained in Sec. 2.3.

3. Consult the appropriate figure from Fig. 4.13, 4.23, 4.33, 4.41, to 4.51 to become informed as to the appearance of the girder before and after testing. In addition, these figures mark the locations of the photographs presented in this report. If a frame appears in dashed lines, the picture was taken from the far side of the girder; if in solid lines, from the near side. Furthermore, the location of the strain rosettes, the strain gages on the transverse stiffeners, the measured diagonals, and the cross sections at which web deflections were recorded are all shown in self-explanatory symbols. All these positions indicated are not the only places where recordings were obtained; they are the ones at which the measurements were taken from which graphs presented in this report were made. Likewise, the presence of a symbol indicating measurements before a later test does not exclude observations with this instrument at an earlier test, but rather indicates to which test the particular graph pertains.

4. For the basic test measurements, select the suitable graphs from the followings for girders E2, E4, E5, G8, and G9 respectively:

- Fig. 4.14, 4.24, 4.34, 4.42, and 4.52 for the state of stress in the web as measured by pairs of strain rosettes.

- Fig. 4.15, 4.25, 4.35, 4.43, and 4.53 for the axial strain in a transverse stiffener.
- Fig. 4.16, 4.26, 4.36, 4.44, and 4.54 for the extensions of the panel diagonals.
- Fig. 4.17, 4.27, 4.37, 4.45, and 4.55 for the web deflections at two different cross sections of the girder.

5. Finally, refer to the photographs of the girder for the failure modes of particular interest. These photographs are:

Girder E2: Figs. 4.18, 4.19, 4.20, 4.21
E4: Figs. 4.28, 4.29, 4.30, 4.31
E5: Figs. 4.38, 4.39
G8: Figs. 4.46, 4.47, 4.48, 4.49
G9: Figs. 4.56, 4.57, 4.58, 4.59

To conclude this section, a summary of all the ultimate loads is given in Table 4.1. Here also are listed the yield, plastic, and critical loads of each test. The difference between the ultimate load P_u and the maximum load P_{max} lies in their definition. Whereas P_u is a static load, the maximum load is recorded during load application; the exact definitions being given in Sec. 2.4.

4.4 Discussion

With the test results given, certain features which are likely to be otherwise overlooked are presented in this section.

In the description of the test setup, concern was expressed over the lack of a well defined test section for each girder. It was feared that failure might take place locally at the loading point where the combination of moment and shear was most severe and where the stress conditions were made obscure by the load application. As the test results show, this concern was unnecessary. At the loading point, the girder elements under compression were braced so that they could strain harden since the compression flange plate was guided by the loading device and the web was braced by the loading stiffeners. The tension flange, being self stabilizing, did not require any special attention.

Although no local failure was developed at the loading point, the details at the ends of the test girders proved to be of more concern. Considering, for instance, the test of girder E₄, one would assume that failure occurred somewhere near midspan, but the actual case was an almost sudden failure of an end panel, Fig. 4.28.

The reason for such a failure is that the tension field action cannot build up to its full extent without a neighboring panel, unless the end post has enough bending rigidity to serve as an anchor for the tension field. The end posts made from a 12WF50 section seemed to be sufficient for a very long panel, $\alpha = 3$, where the tension field action is less pronounced. However, for a shorter panel, $\alpha = 1.5$, the end post collapsed in the manner shown in Fig. 4.7. Of course the web slenderness also influences the end failure. For girder G9 having an extremely thin web, the shear resistance depended almost entirely on tension field action and end failure occurred also for a stiffener spacing $\alpha = 3$, Fig. 4.57. When this happened again at the other girder end, two steel plates were tightly clamped to the outstanding web as shown in Fig. 4.58. Thus, the shear strength of G9-T2 could be increased 30% as born out by the corresponding points in the load-deflection curve, where load Nos. 17 and 20A are the ultimate loads before and after the reinforcement respectively. In order to distinguish between true tests and premature failures due to insufficient end detail, the latter are marked in Table 4.1 with subscript "e". A detailed study of this end post failure will be given in the theoretical report.

Disregarding the premature failure in the end panels, it can be seen that for girders subjected to both shear and bending, the shear strength was hardly affected by the bending moment. Conversely, the bending strength was not affected by the shear force in the case of Girder G5 which failed in a panel with closer stiffener spacing, $a = 0.75$, rather than in one with $a = 1.5$. The solution of the problem of interaction between bending and shear is presented in Ref. 7 and will be treated again in the forthcoming theoretical report.

Briefly, the highlights revealed by the tests on this series of girders can be summarized as follows:

- Failure of a properly proportioned girder is unlikely to occur directly at the point of load application, although the bending moment is highest there.
- The design of girder ends requires special attention if the same shear strength is desired in an end panel as within the girder.
- The presence of bending moment little affects shear strength, that is, the interaction between bending and shear is not a pronounced one.

* * *

*

In concluding, it should be recalled that the objective of the entire investigation was to study the problem of web buckling. These tests, therefore, are of both academic and practical value.

The academic value of this investigation is that it demonstrates convincingly that the web buckling theory is unable to predict the strength of plate girders with slender webs. Also the postbuckling strength of girders cannot be simply expressed on the basis of the critical stress as is often expected, that is, the strength of plate girders is not a function of the web slenderness ratio alone. Furthermore, these tests led to a new basis for an ultimate strength prediction.

The practical value is that, besides obtaining solutions to some detailing problems, a new design specification can be drafted with which more economical girders can be built. For example, in view of the existing specification in this country, the bending girder tests clearly indicate that the domain of web slenderness ratios above 170, covered so far only by girders with longitudinal stiffeners, can be opened to plate girders with only transverse stiffeners. The increase in shear strength, as explained by the tension field action, permits either a saving in web area or an increase of transverse stiffener spacings. The third series of the tests, containing girders

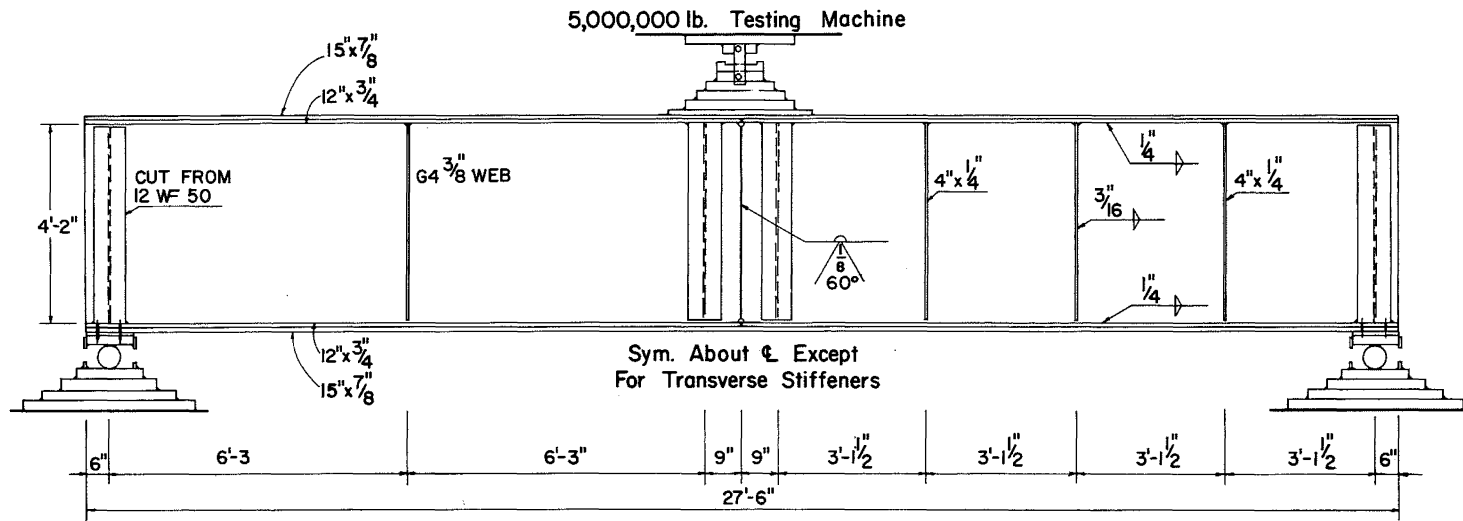
with web slenderness ratios as low as one hundred, directly suggests a liberation of the web slenderness limitations of unstiffened plate girders.

Finally, concerning this report, it is hoped that it will serve an additional purpose in providing information on the behavior of built up members, such as plate girders, which is not discussed in standard text books or specification manuals.

Table 4.1

Summary of Reference and Experimental Loads

Girder	Test	Theoretical			Experimental	
		P _{cr} (kips)	P _y (kips)	P _p (kips)	P _u (kips)	P _{max.} (kips)
E1	T1	332	826	920	555	576
	T2	402	826	920	580	598
	T3	415	905	920	(634)e	656
	T4	506	826	920	(684)r	710
E2	T1	570	716	855	755	774
	T2	584	716	855	757	810
E4	T1	445	880	905	(595)e	616
	T2	513	658	691	634	670
	T3	517	639	666	645	700
E5	T1	314	248	367	350	359
	T2	322	358	386	360	364
G8	T1	41.5	280	368	170	180
	T2	56.4	410	434	(200)e	207
	T3	48.3	280	368	233	241
	T4	57.3	280	368	(259)r	273
G9	T1	12.9	264	354	(96)e	101
	T2	16.8	324	336	(150)e	155
	T3	15.5	264	354	158	162



Typical also for Girders E1, E2, E5, G8 & G9

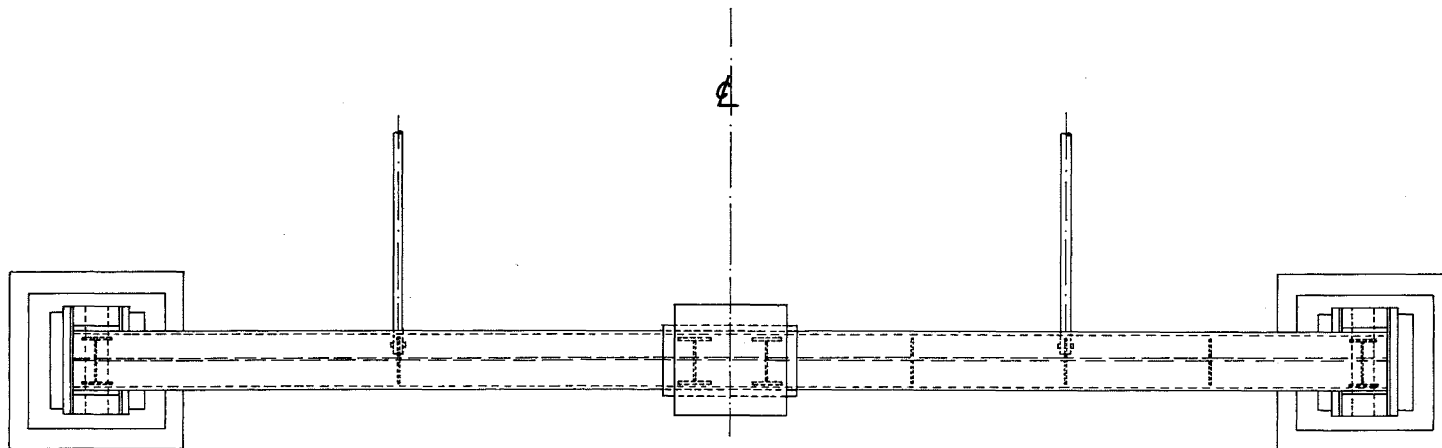


Fig. 4.1 Plate Girder E4 with Test Setup

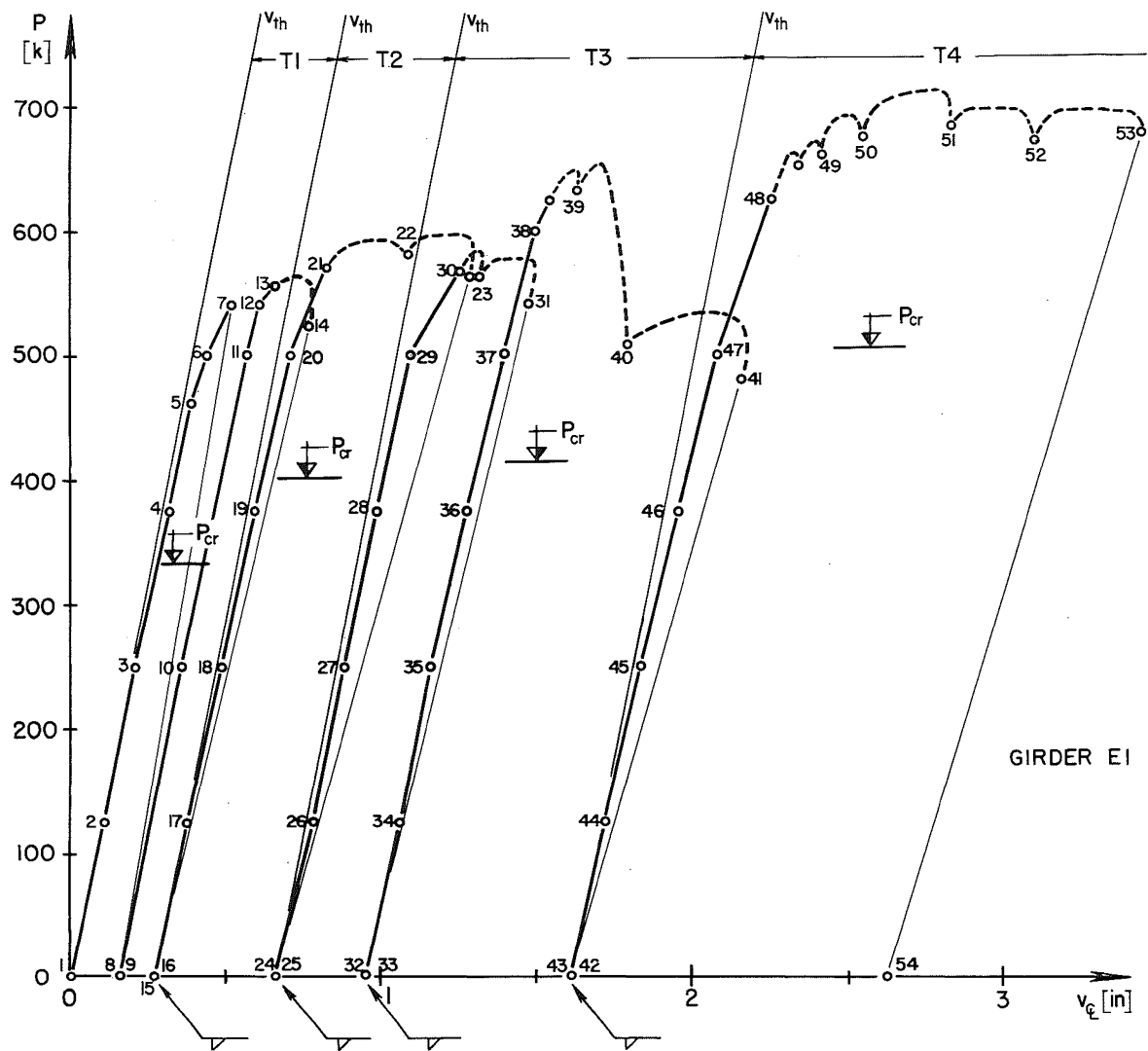


Fig. 4.2 Load-Deflection Curve, Girder E1

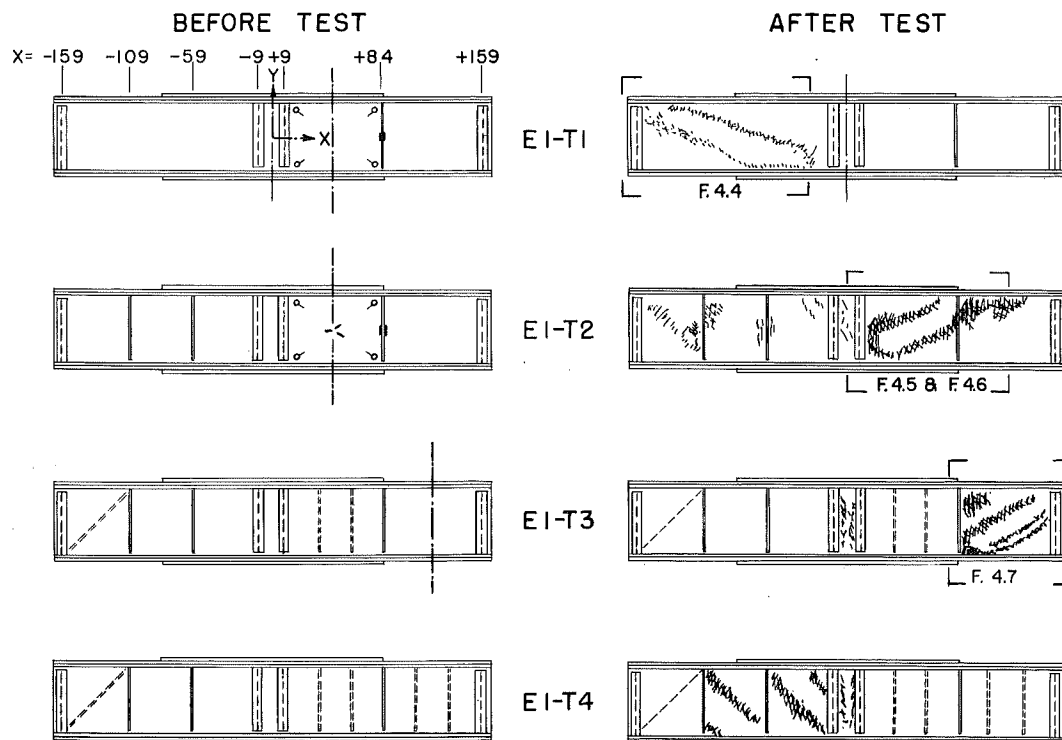


Fig. 4.3 Girder EI Before and After Tests

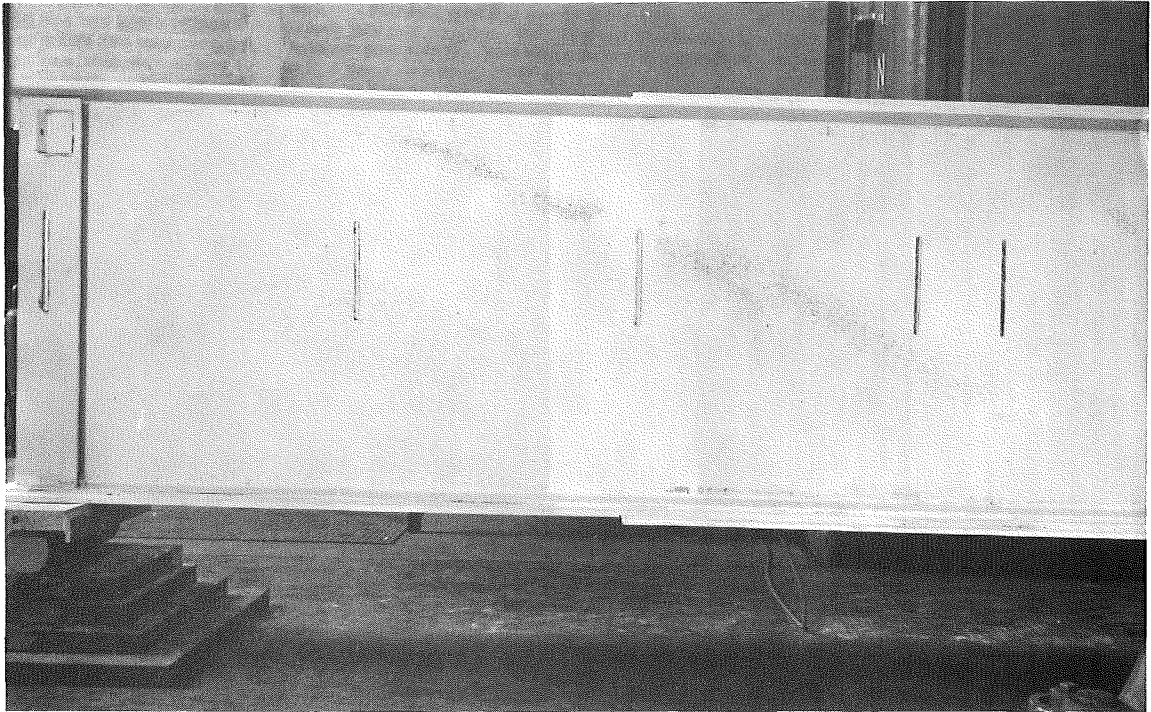


Fig. 4.4 Shear Failure, EI-T1

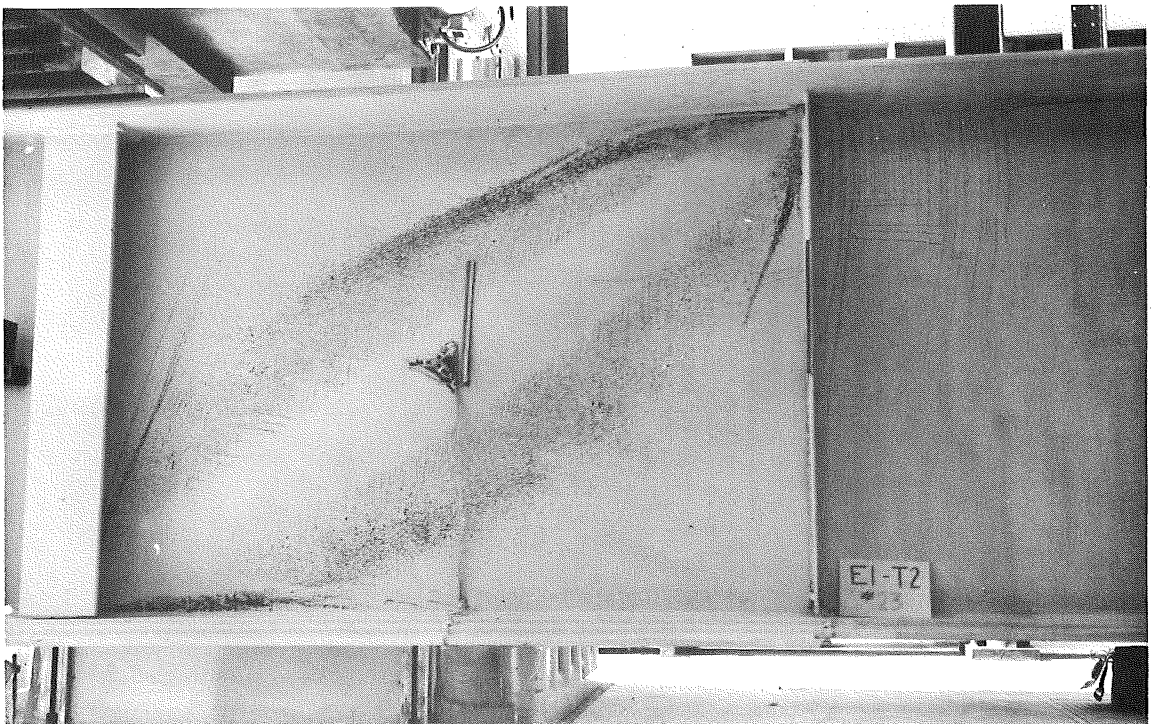


Fig. 4.5 Shear Failure, EI-T2, Near Side

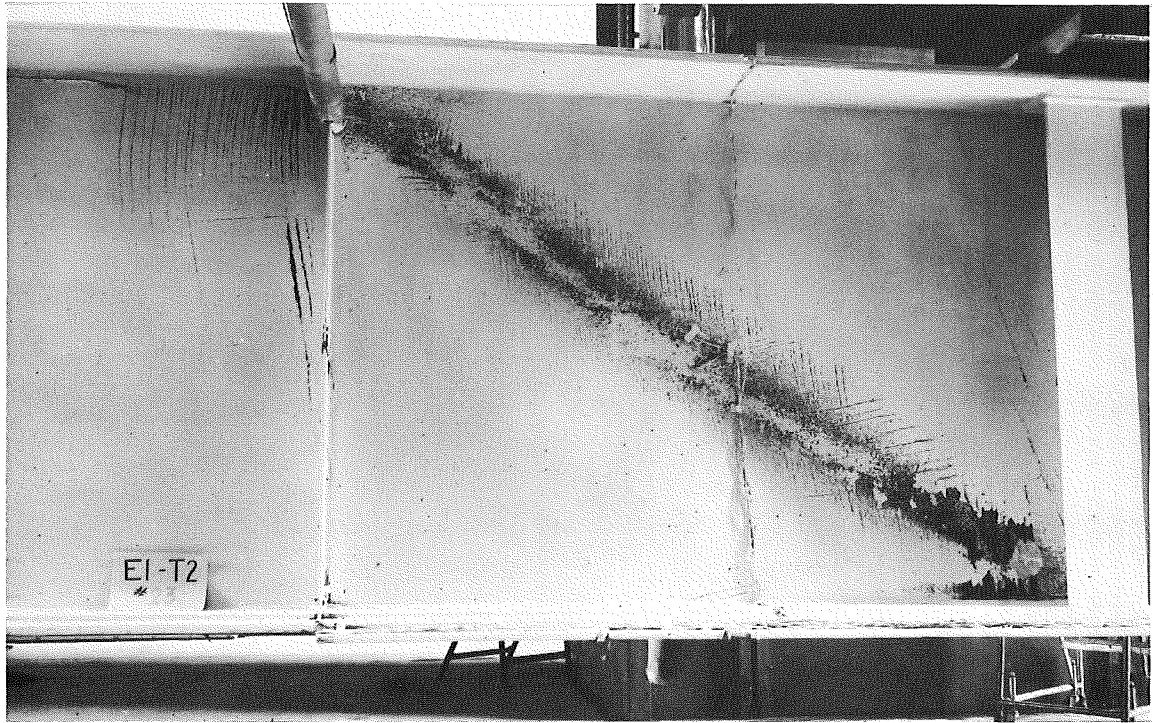


Fig. 4.6 Shear Failure, EI-T2, Far Side

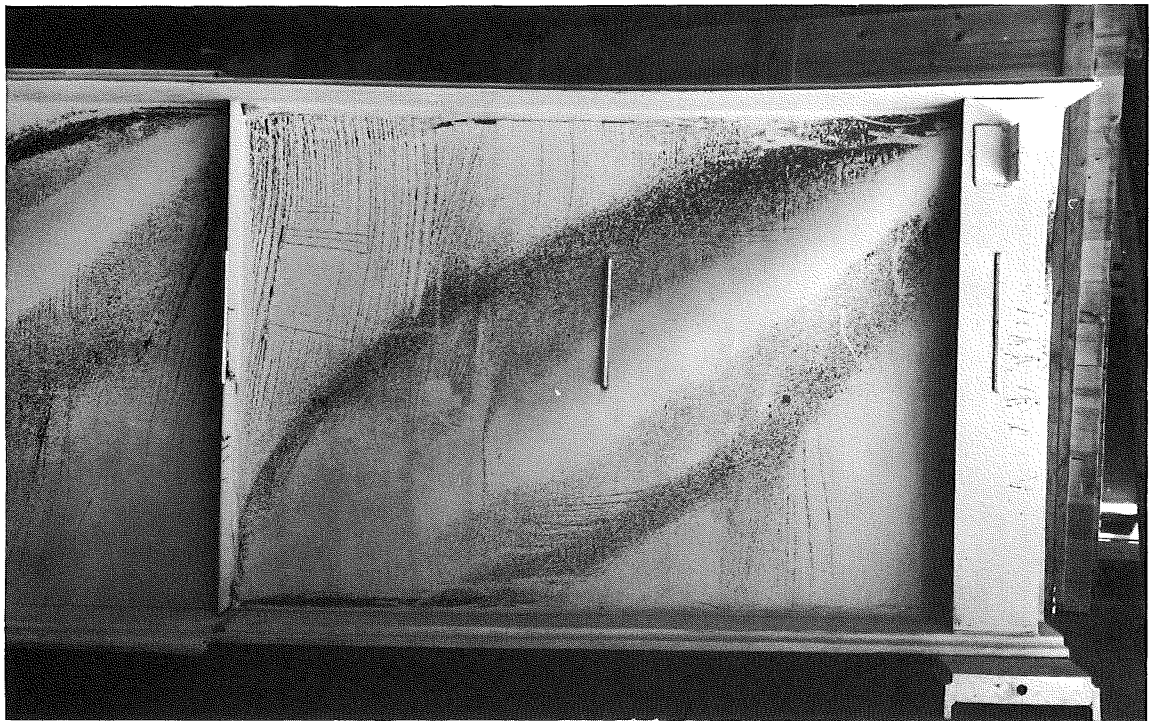


Fig. 4.7 Typical End Panel Failure of Plate Girder (EI)

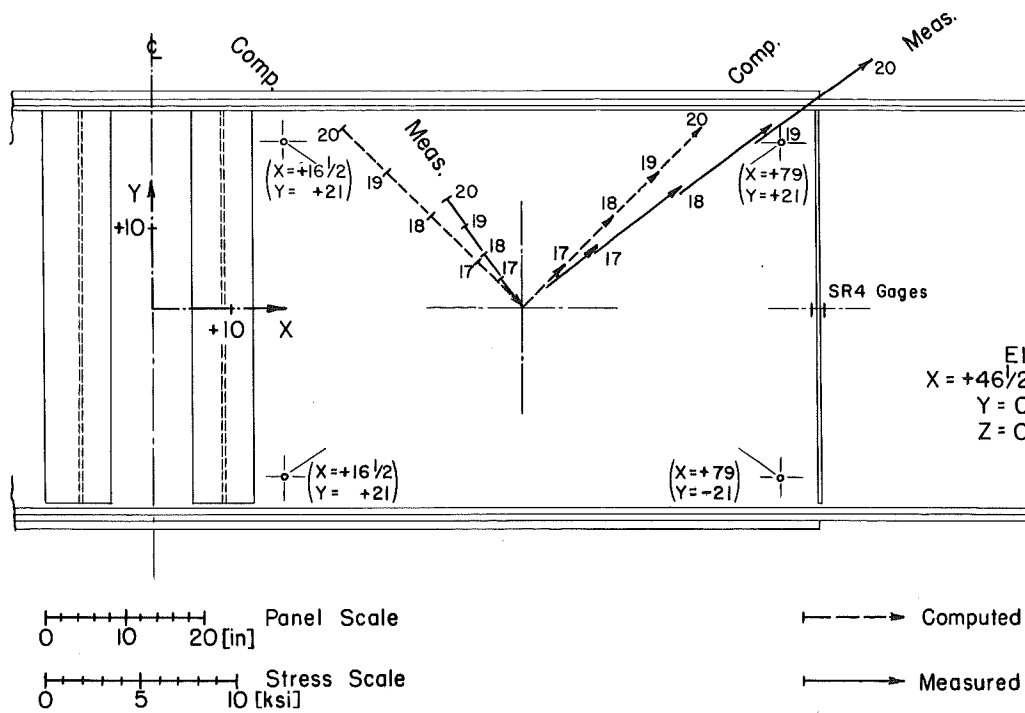


Fig. 4.8 Principal Stresses at Panel Center, Girder E1

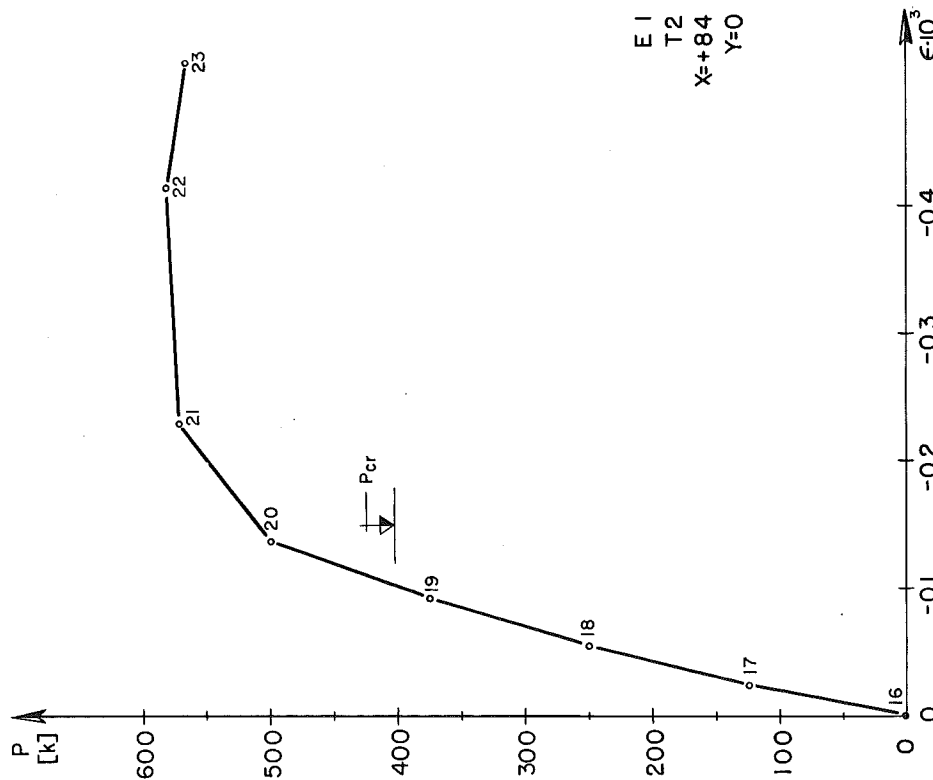


Fig. 4.9 Axial Strain in a Transverse Stiffener, Girder E1

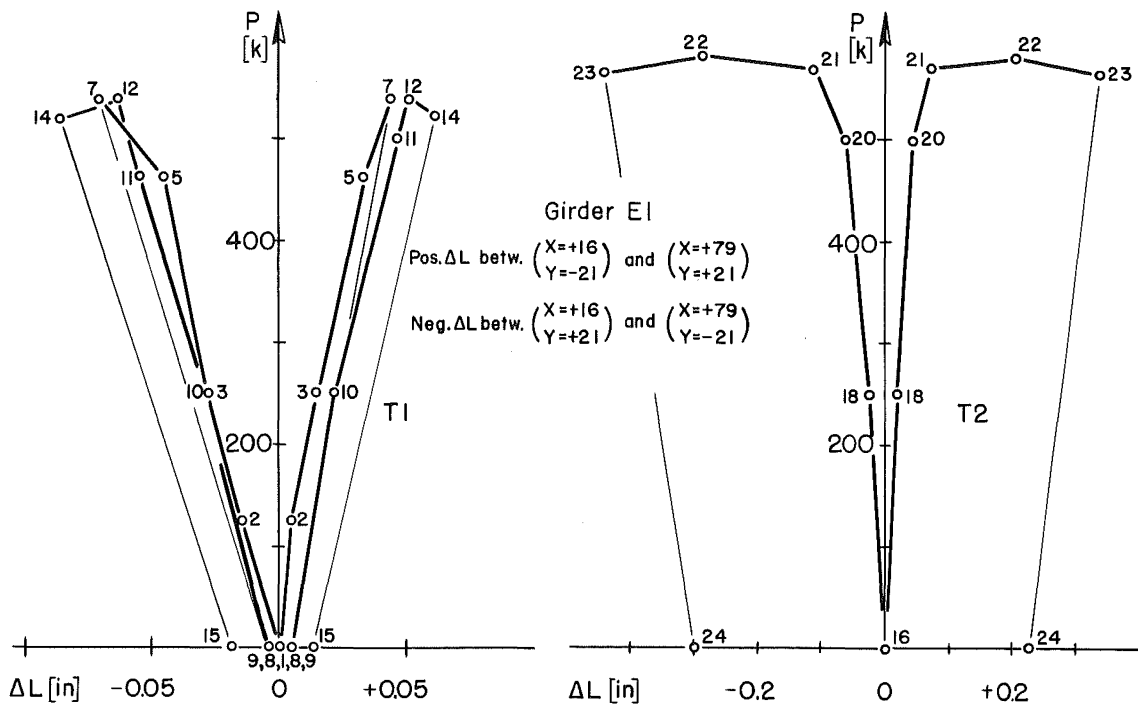


Fig. 4.10 Displacements in the Direction of Panel Diagonals, Girder EI

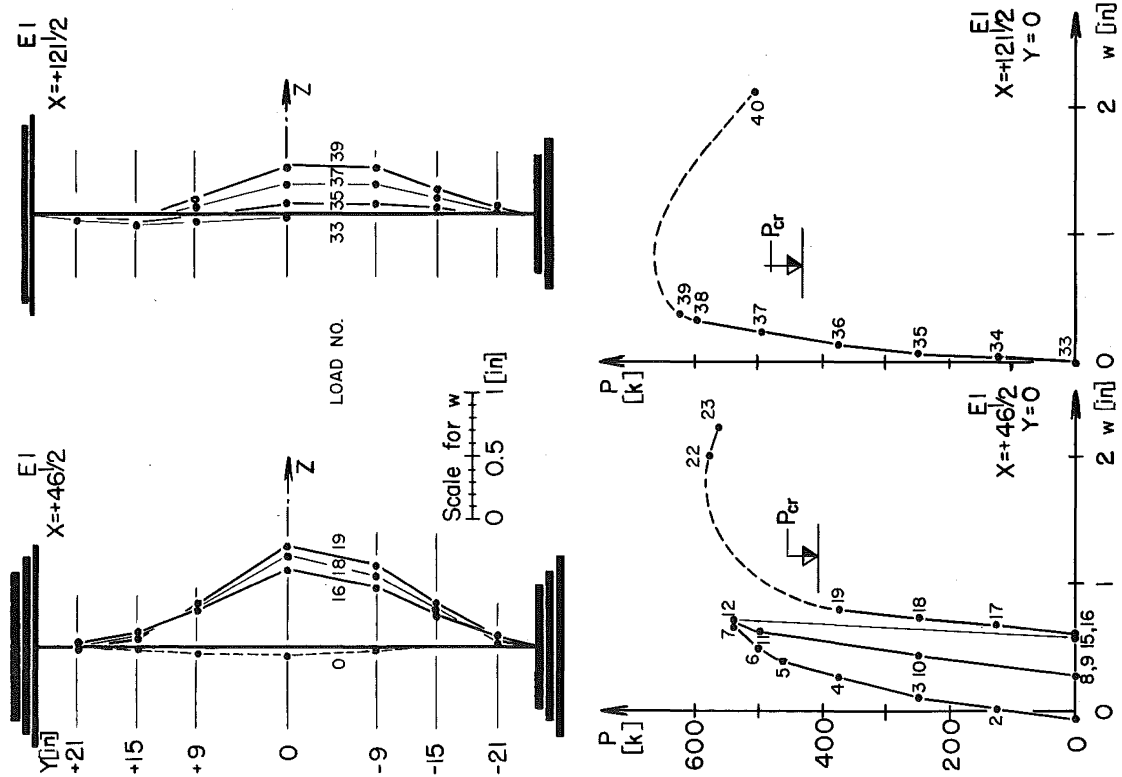


Fig. 4.11 Web Deflections, Girder EI

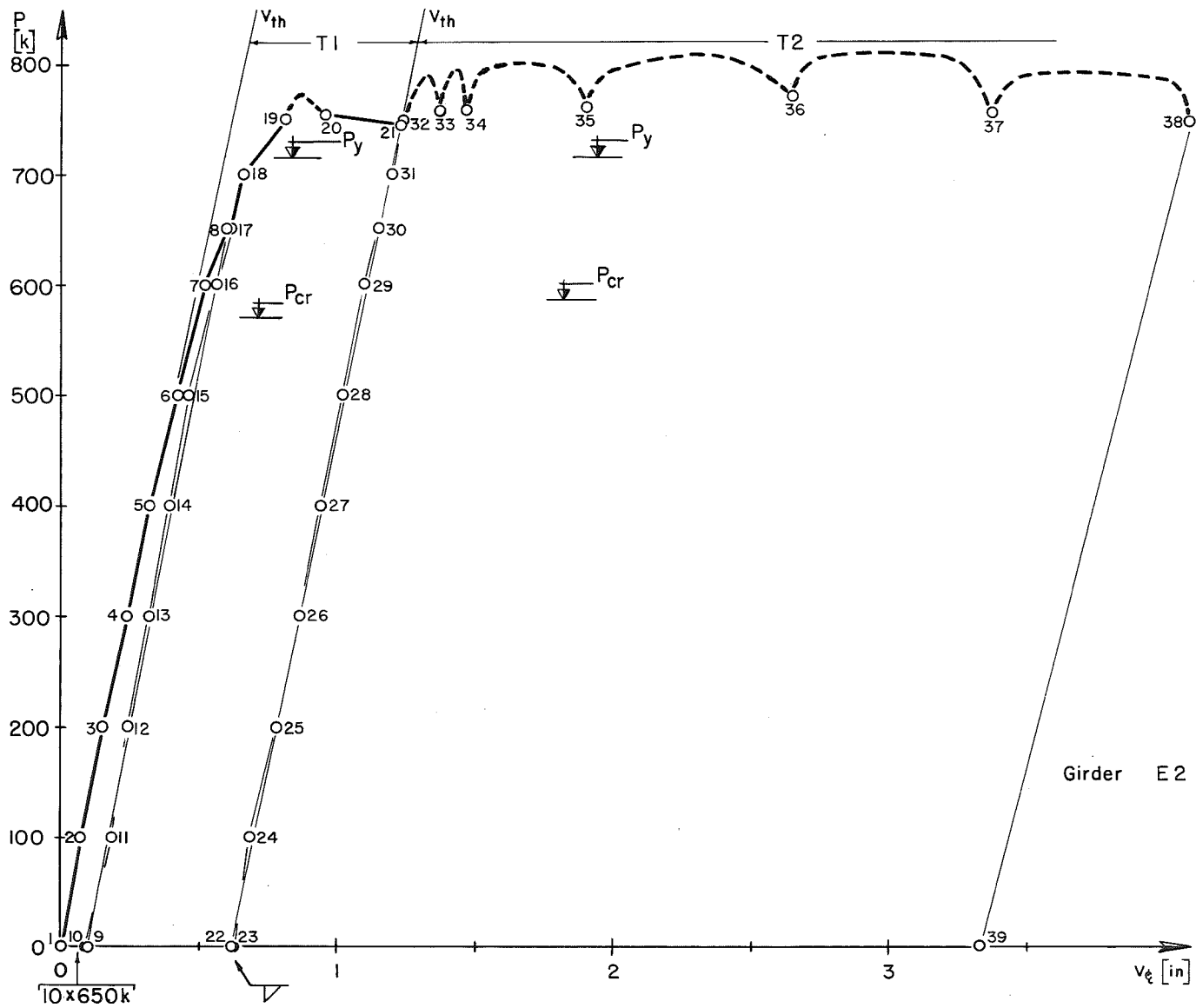


Fig. 4.12 Load-Deflection Curve, Girder E2

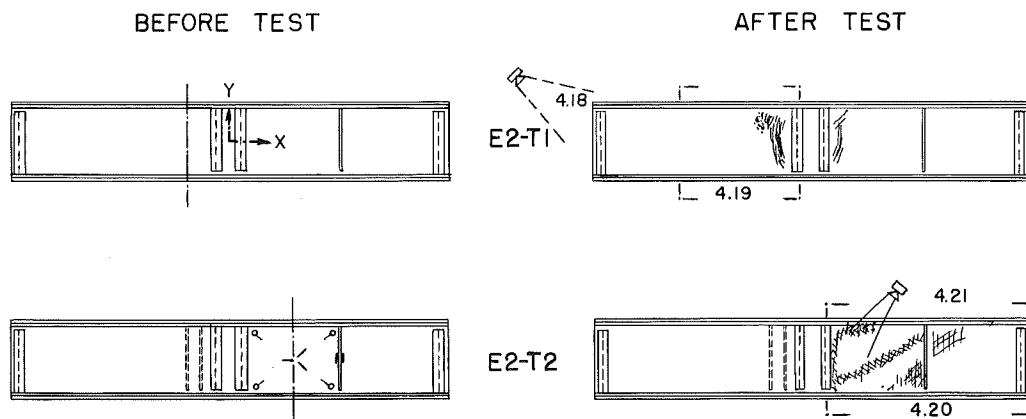


Fig. 4.13 Girder E2 Before and After Tests

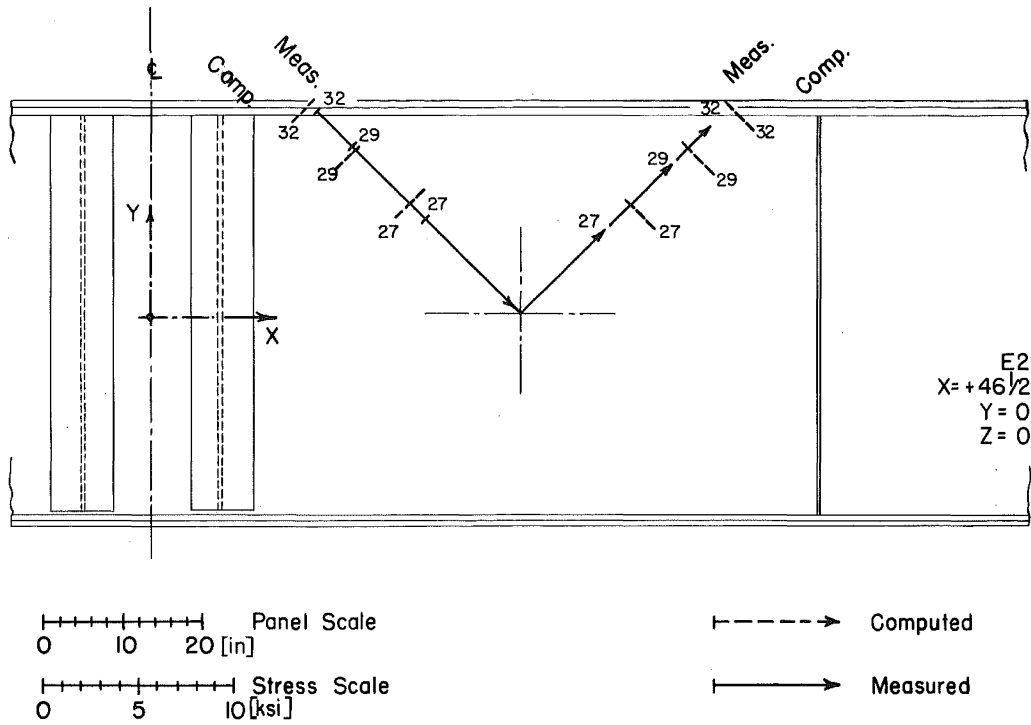


Fig. 4.14 Principal Stresses at Panel Center, Girder E2

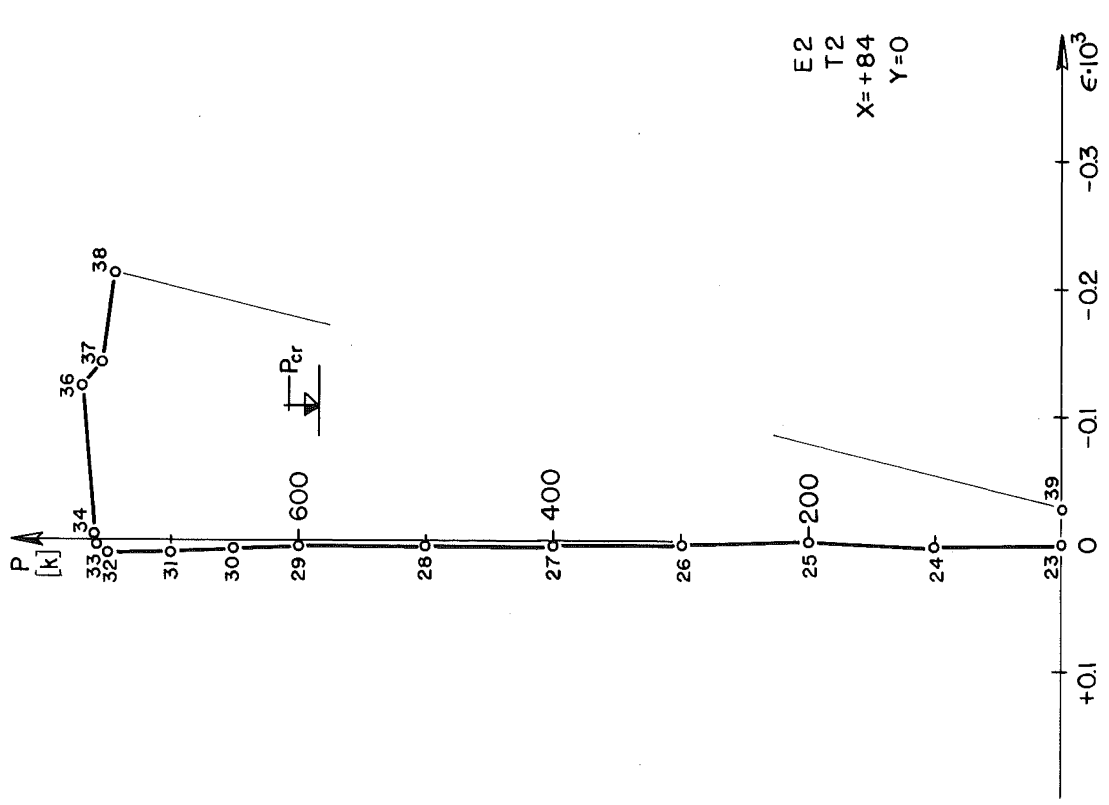


Fig. 4.15 Axial Strain in a Transverse Stiffener, Girder E2

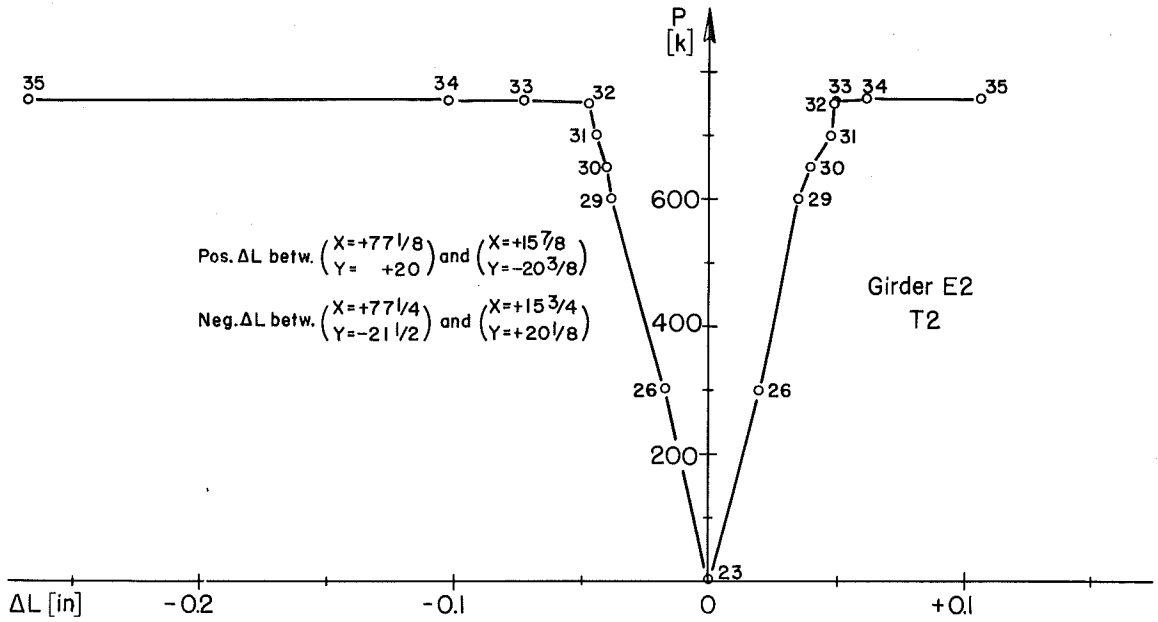


Fig. 4.16 Displacements in the Direction of Panel Diagonals, Girder E2

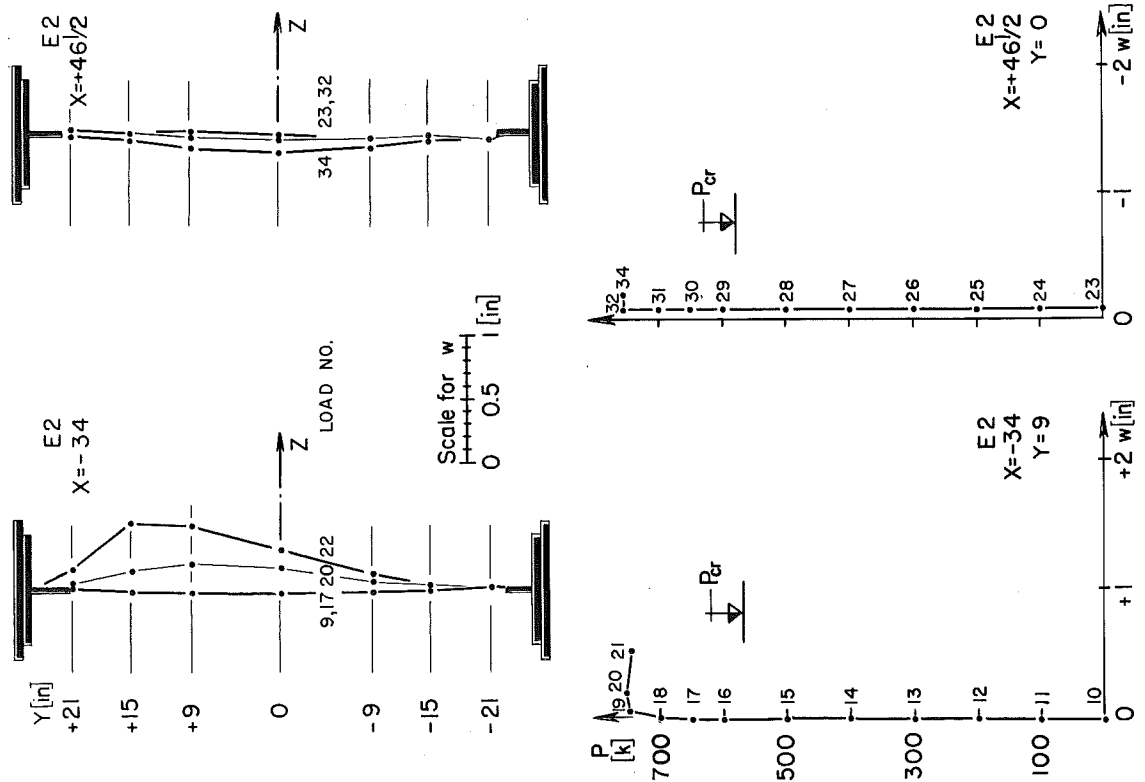


Fig. 4.17 Web Deflections, Girder E2

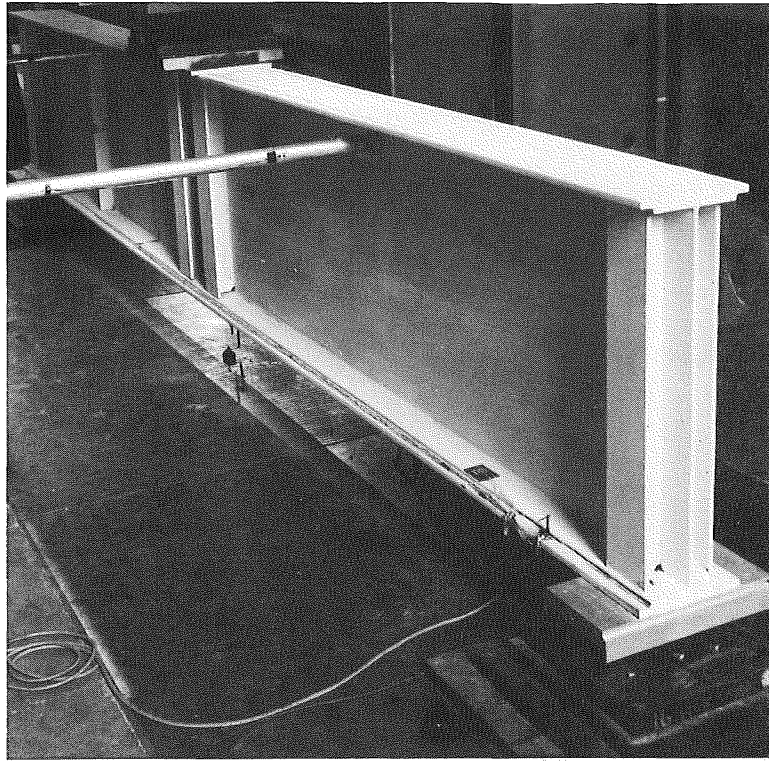


Fig. 4.18 Girder E2 at Ultimate Load

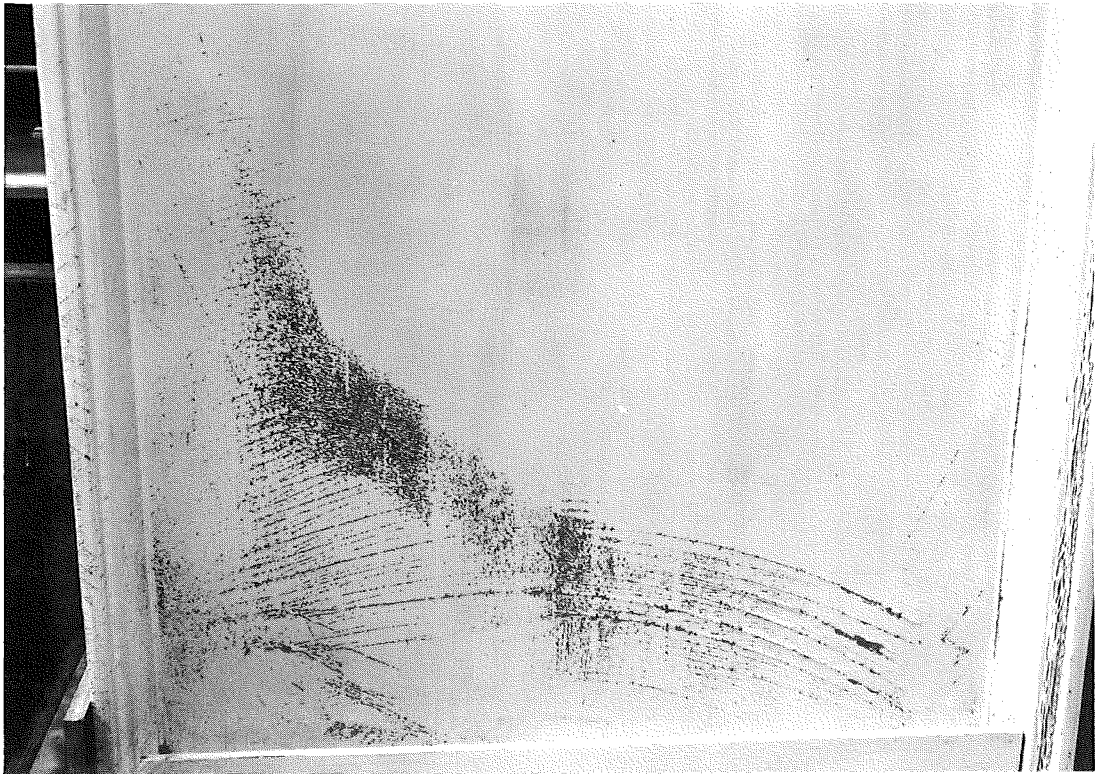


Fig. 4.19 Detail of Failed Section, Girder E2, Test T1

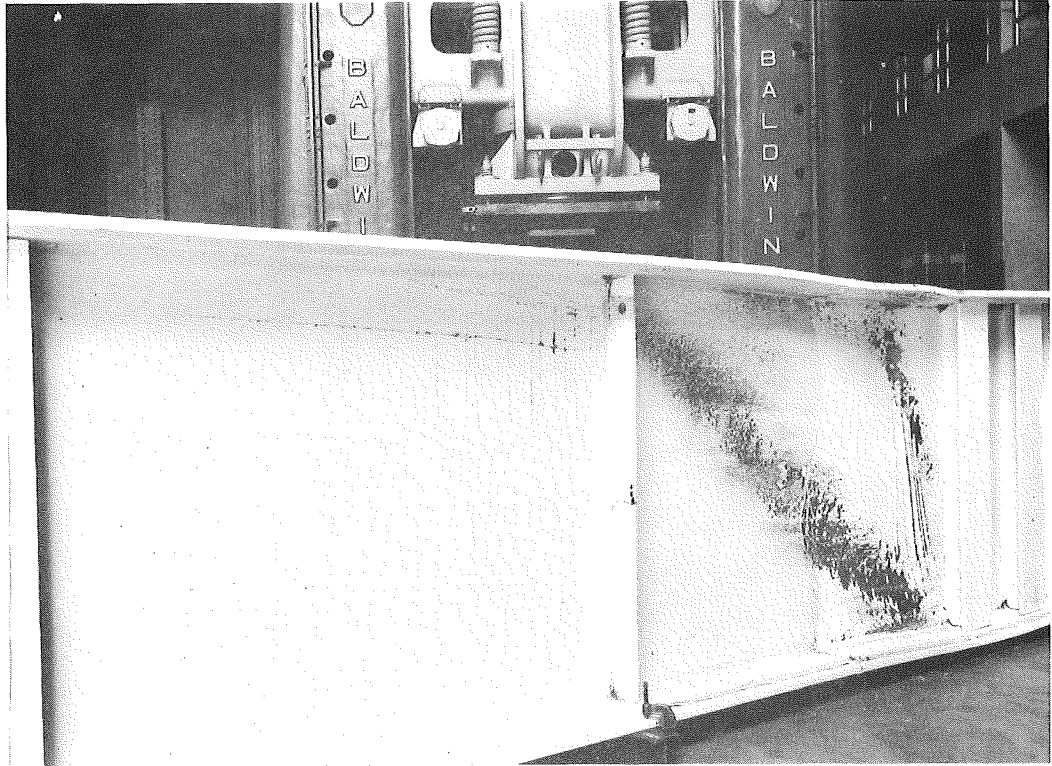


Fig. 4.20 Appearance of Girder E2 After Testing (T2)



Fig. 4.21 Typical Stiffener Detail at Tension Flange (E2-T2)

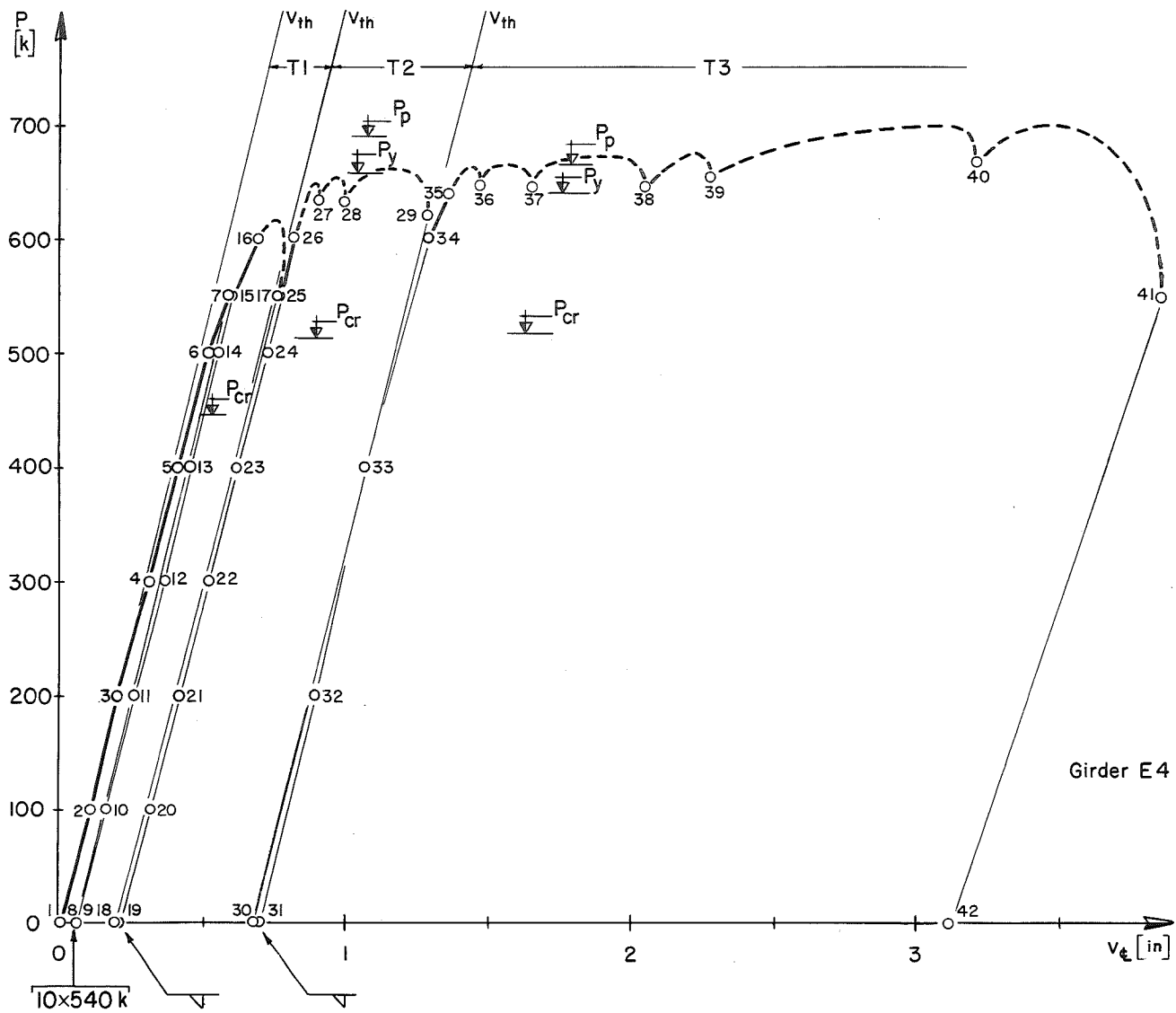


Fig. 4.22 Load-Deflection Curve, Girder E4

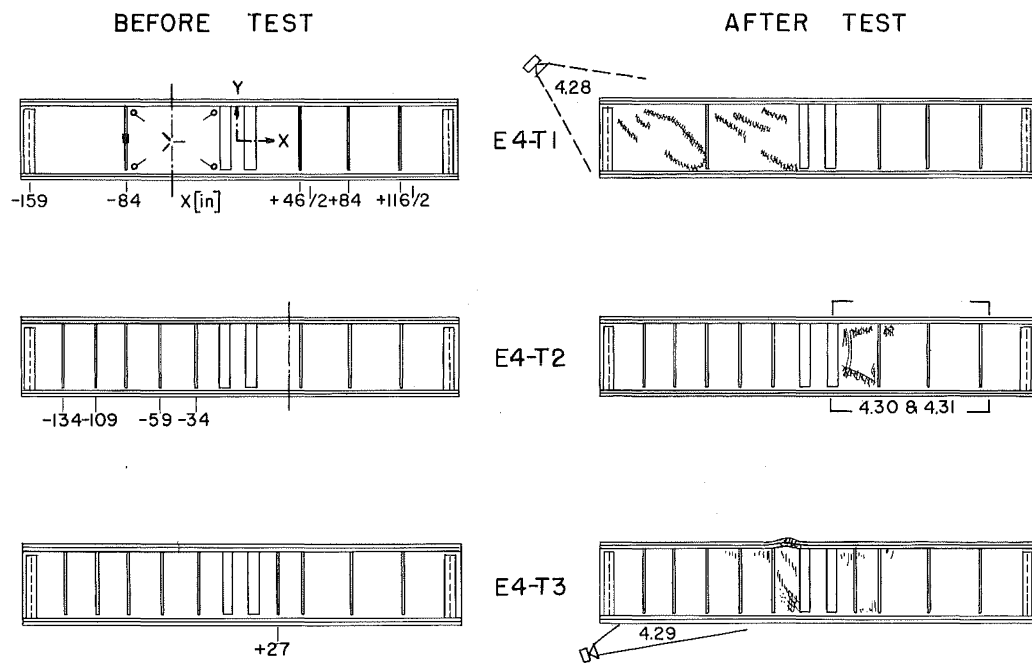


Fig. 4.23 Girder E4 Before and After Tests

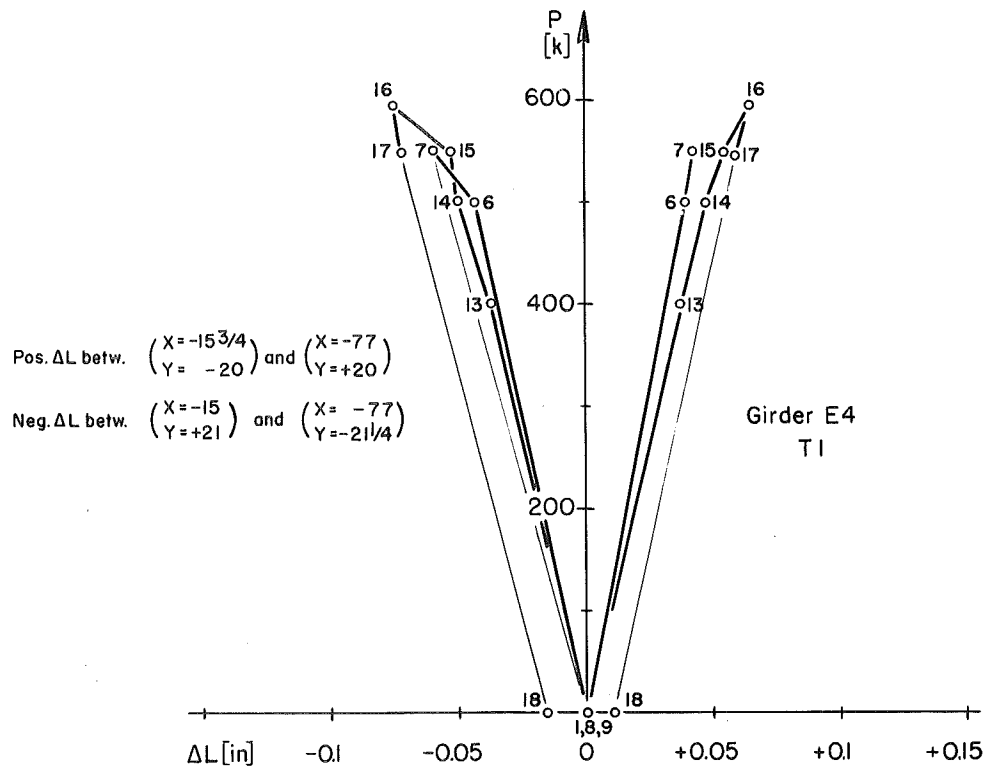


Fig. 4.26 Displacements in the Direction of Panel Diagonals, Girder E4

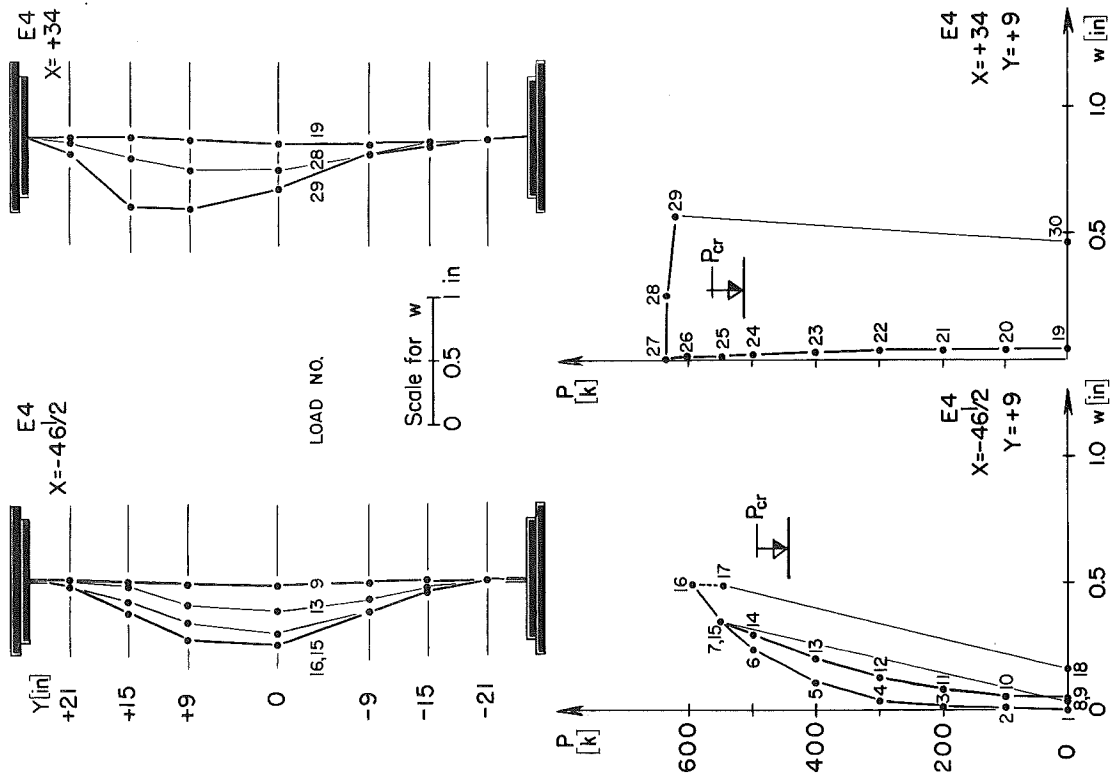


Fig. 4.27 Web Deflections, Girder E4

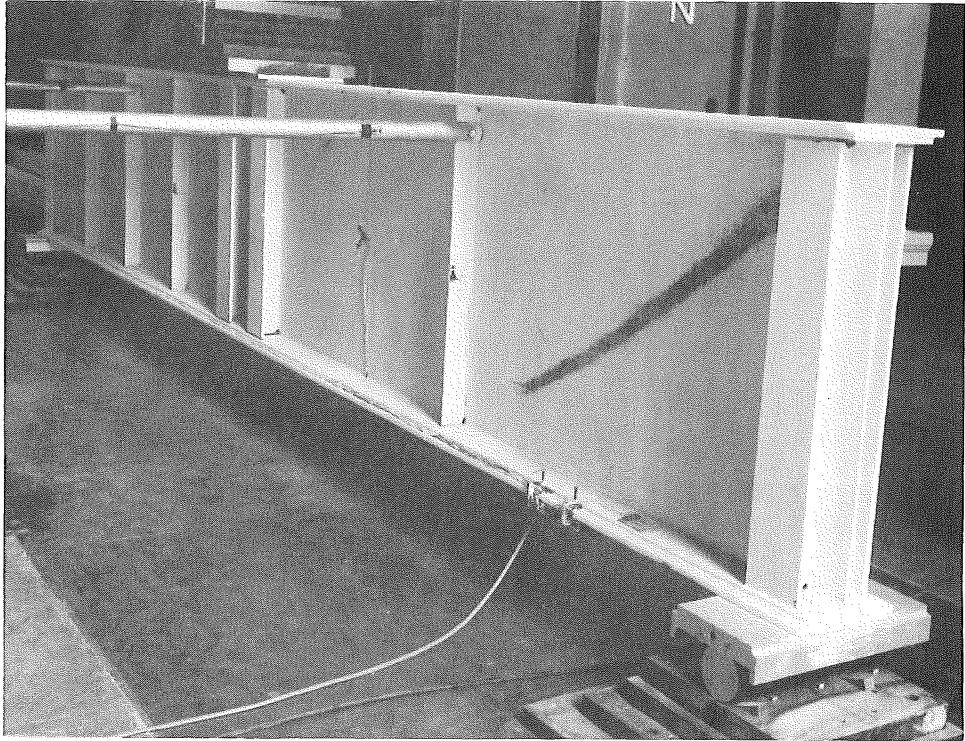


Fig. 4.28 Premature Failure in End Panel, Girder E4

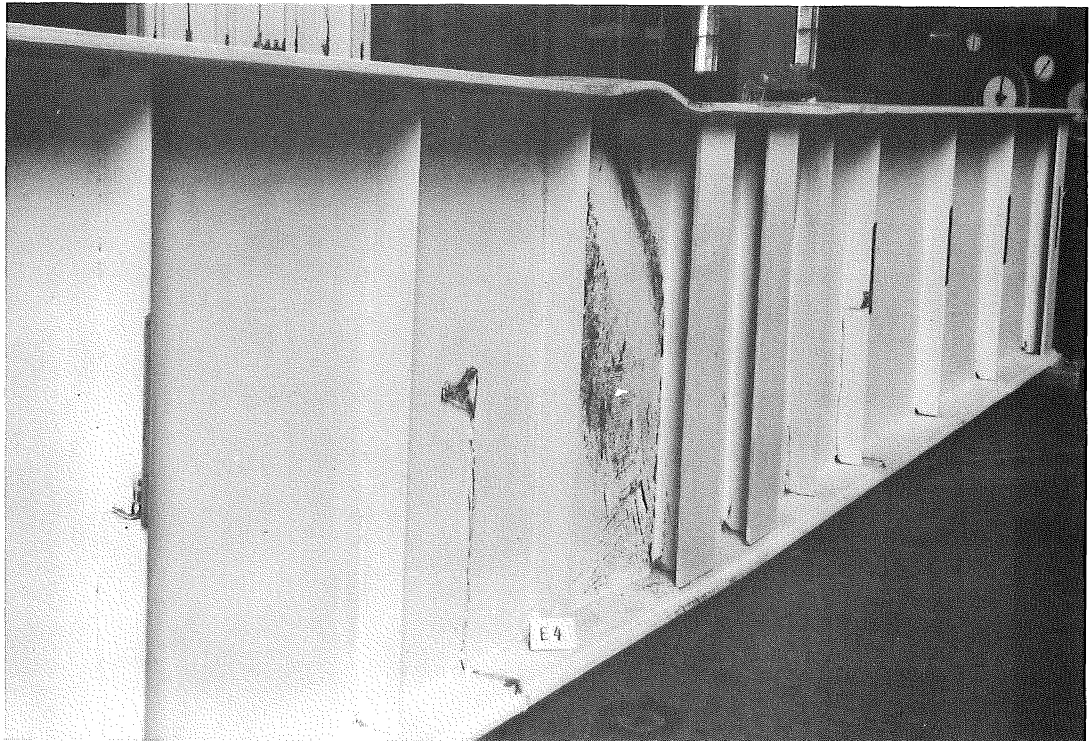


Fig. 4.29 Girder E4, After Testing

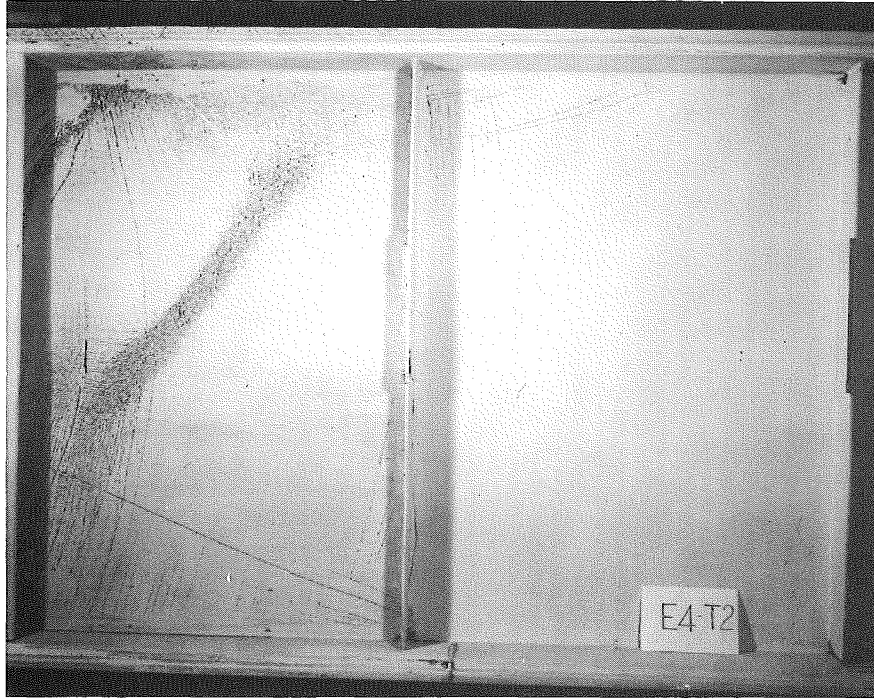


Fig. 4.30 Failure of Girder E4 in Test T2, Near Side

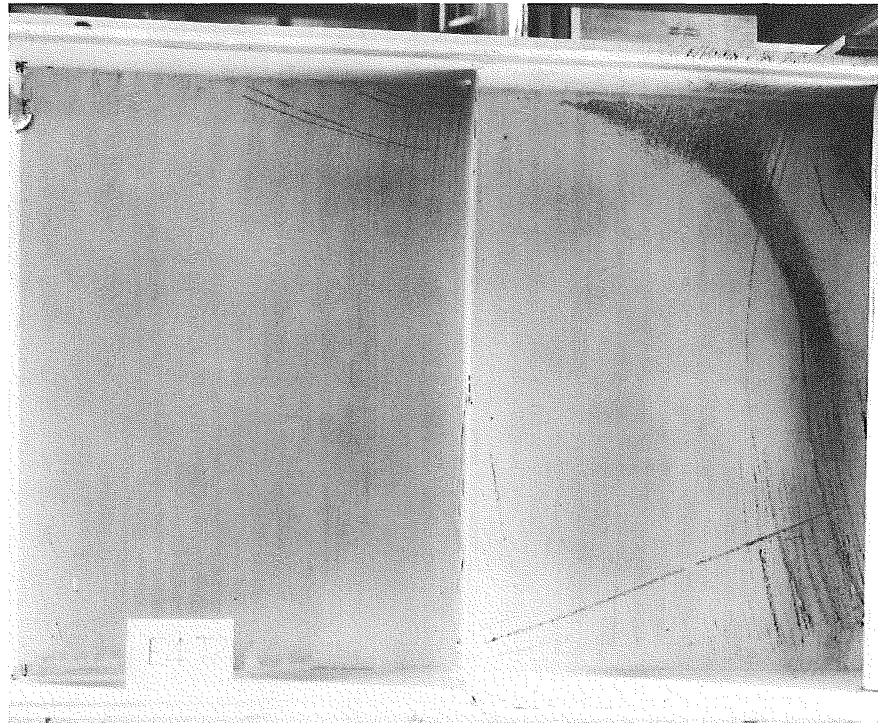


Fig. 4.31 Failure of Girder E4 in Test 2, Far Side

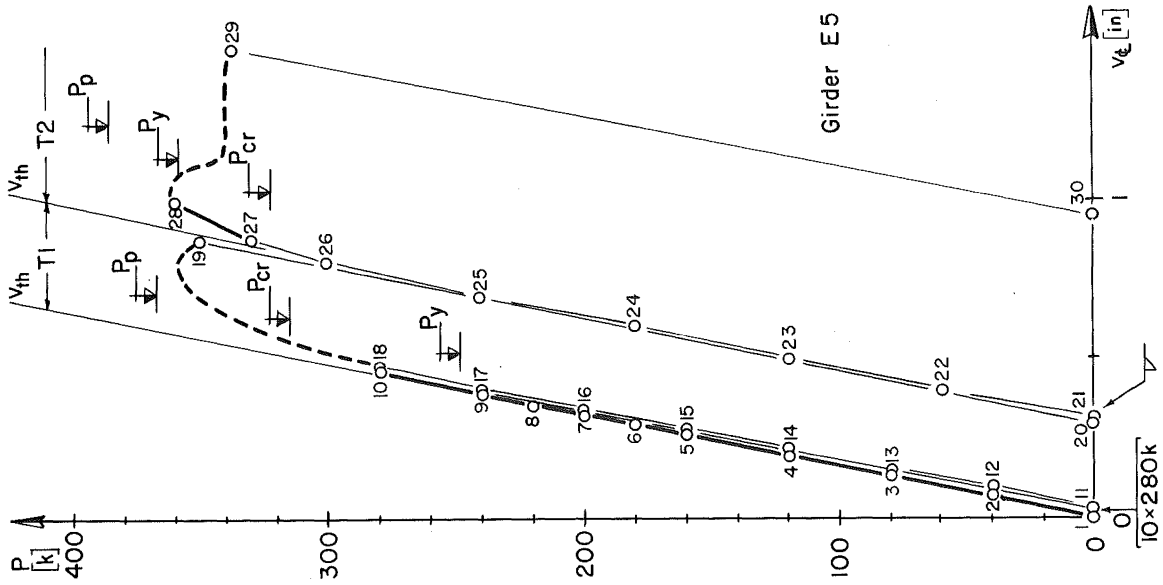


Fig. 4.32 Load-Deflection Curve, Girder E5

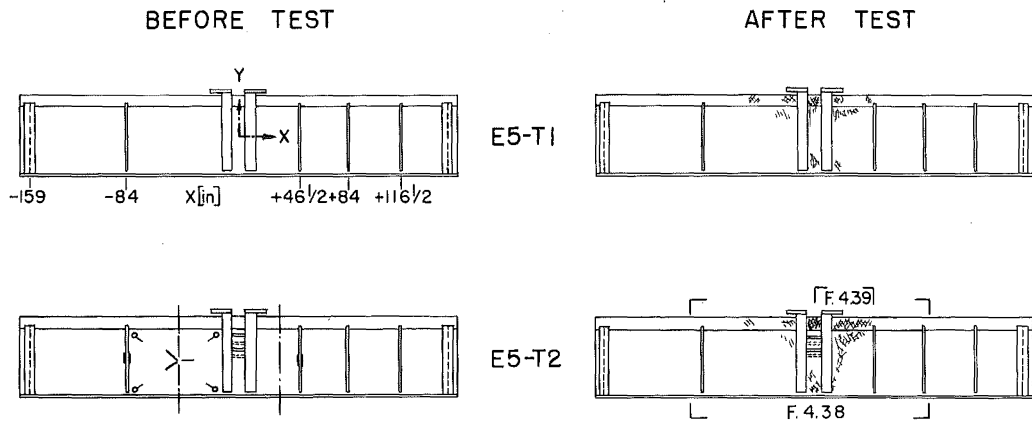


Fig. 4.33 Girder E5 Before and After Tests

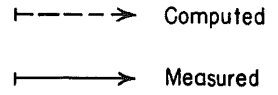
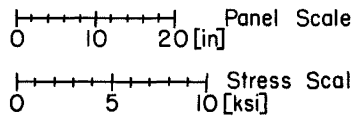
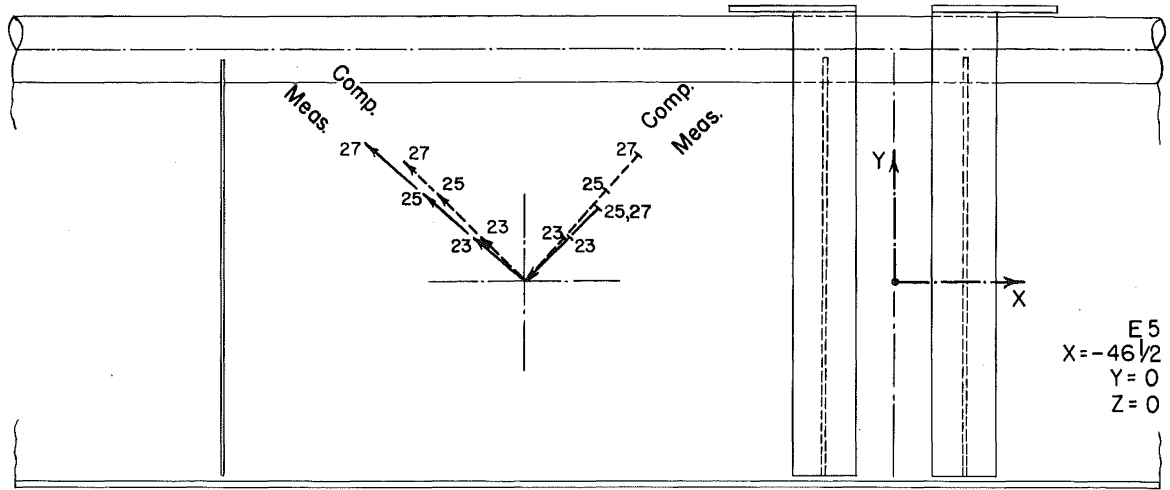


Fig. 4.34 Principal Stresses at Panel Center, Girder E5

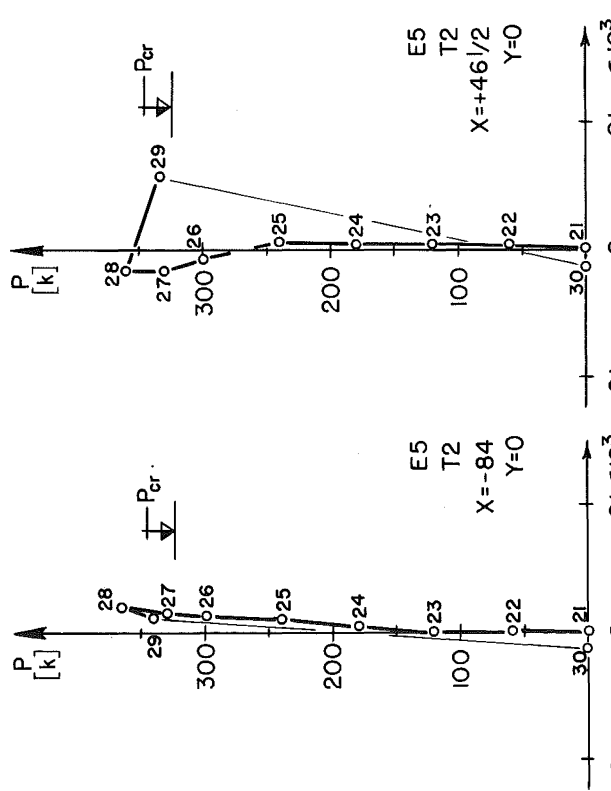


Fig. 4.35 Axial Strain in a Transverse Stiffener, Girder E5

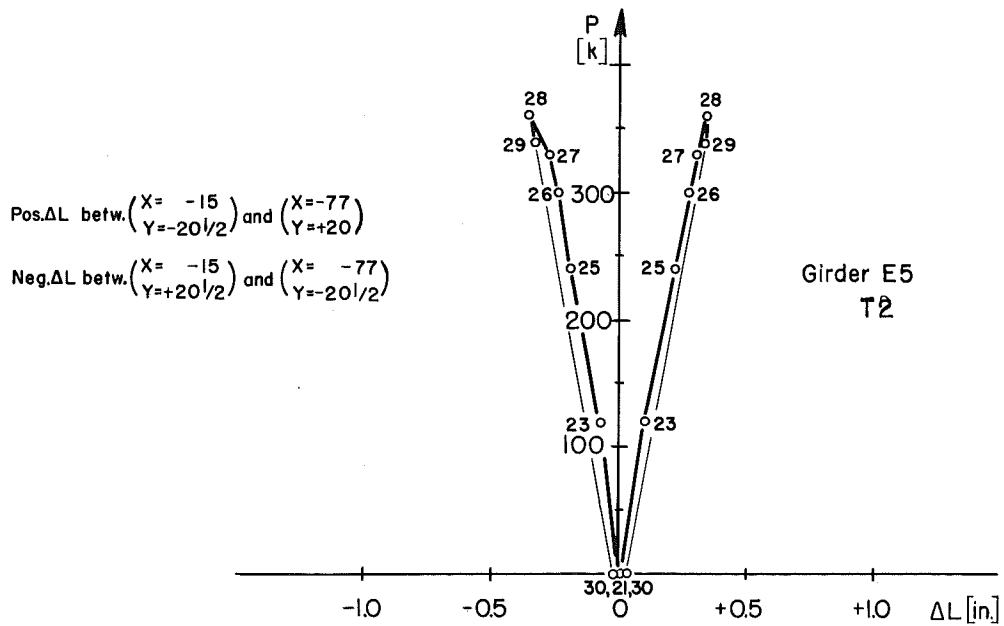
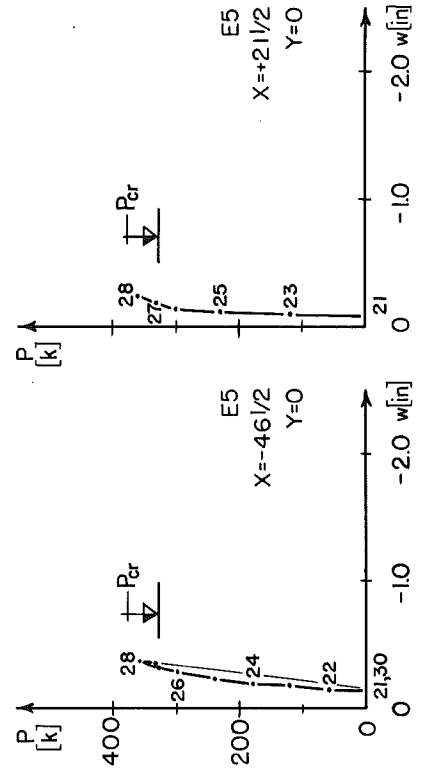
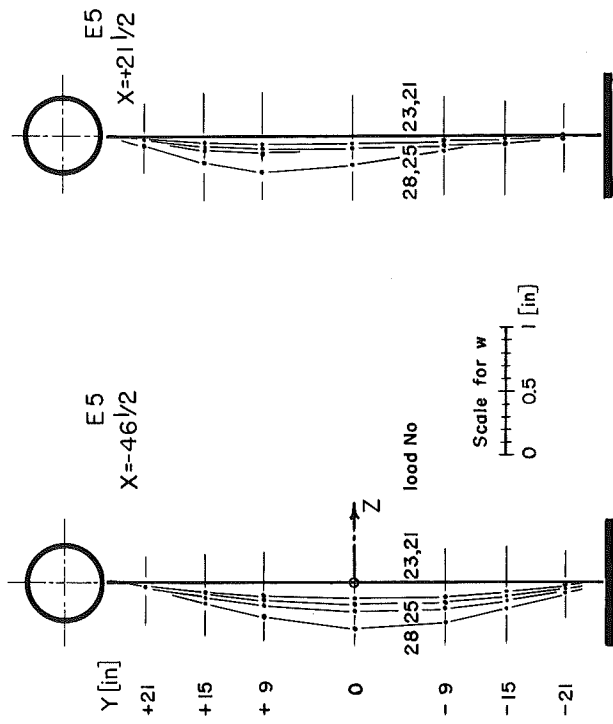


Fig. 4.37 Web Deflections, Girder E5

Fig. 4.36 Displacements in the Direction of Panel Diagonals, Girder E5

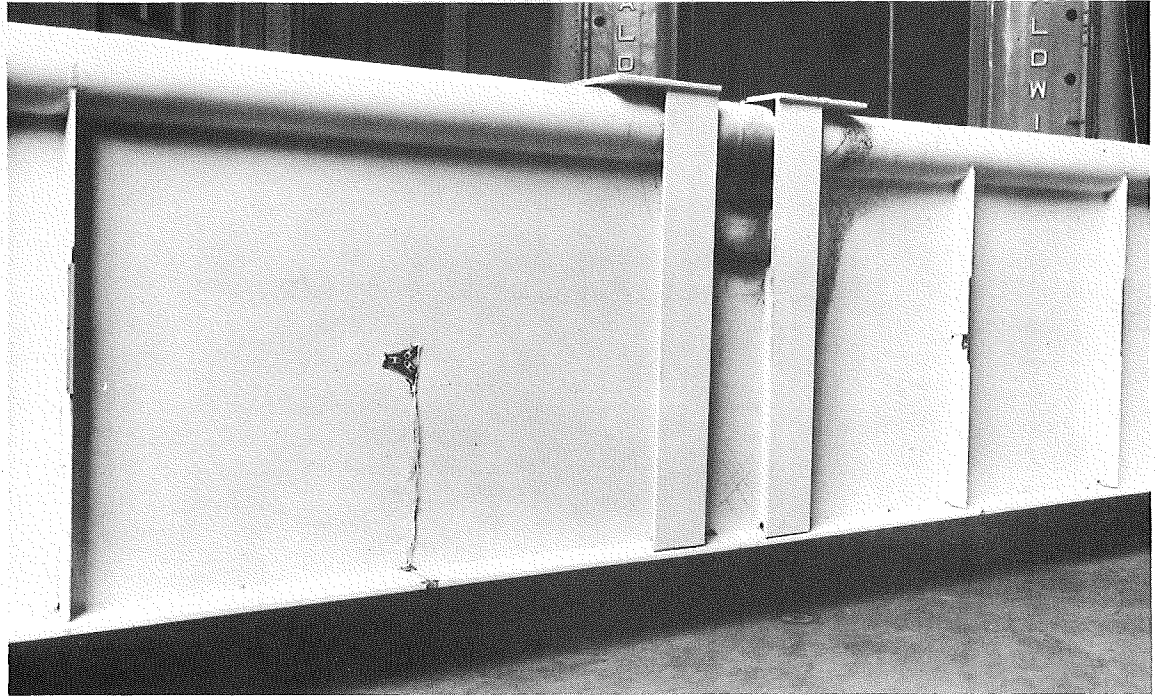


Fig. 4.38 Appearance of Girder E5 after Testing

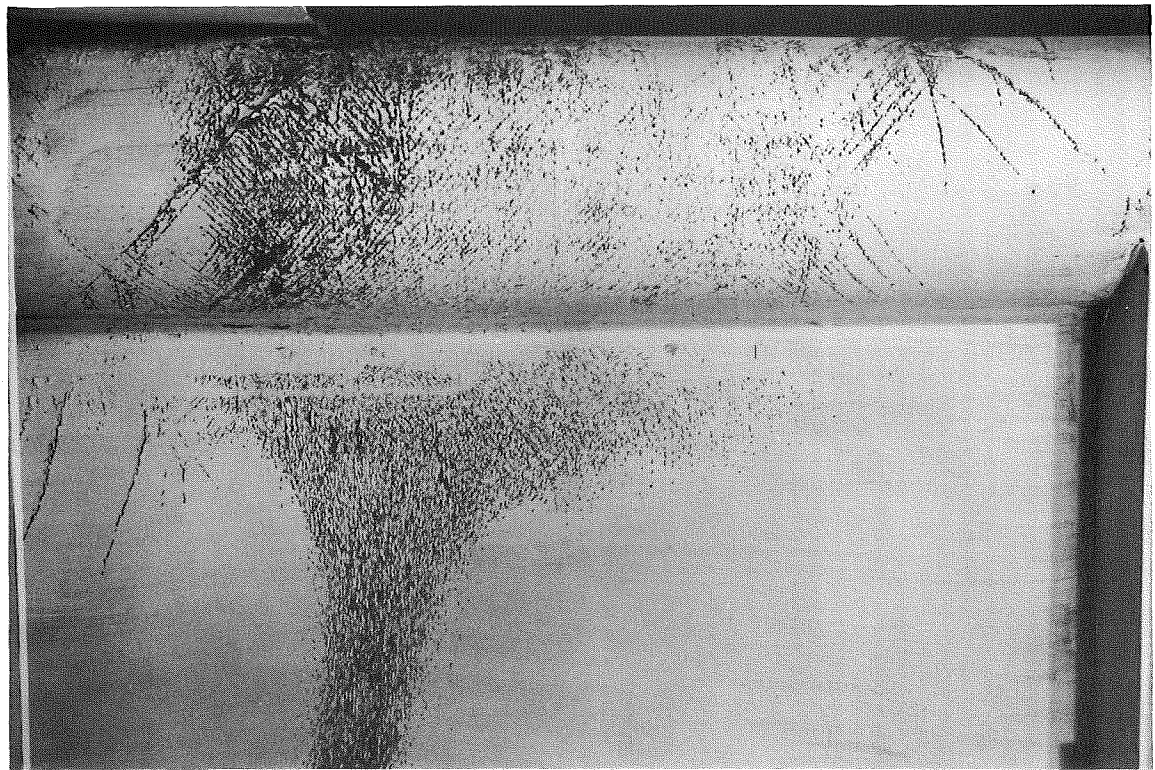


Fig. 4.39 Detail of Failure, Girder E5, Test T2

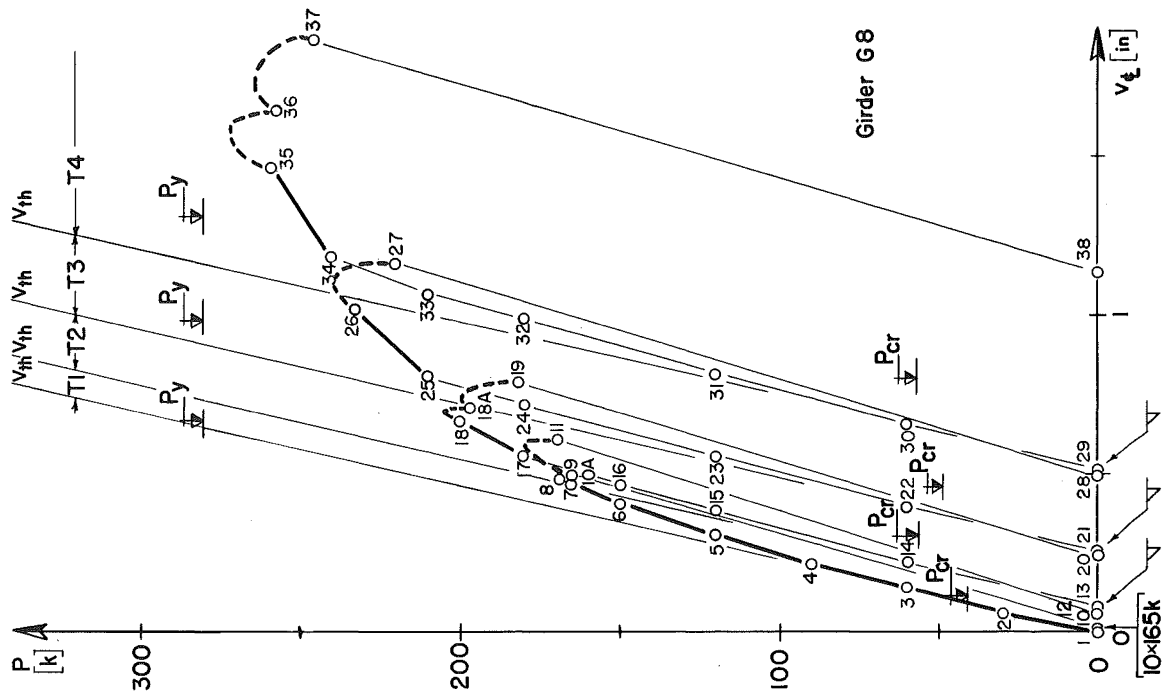


Fig. 4.40 Load-Deflection Curve, Girder G8

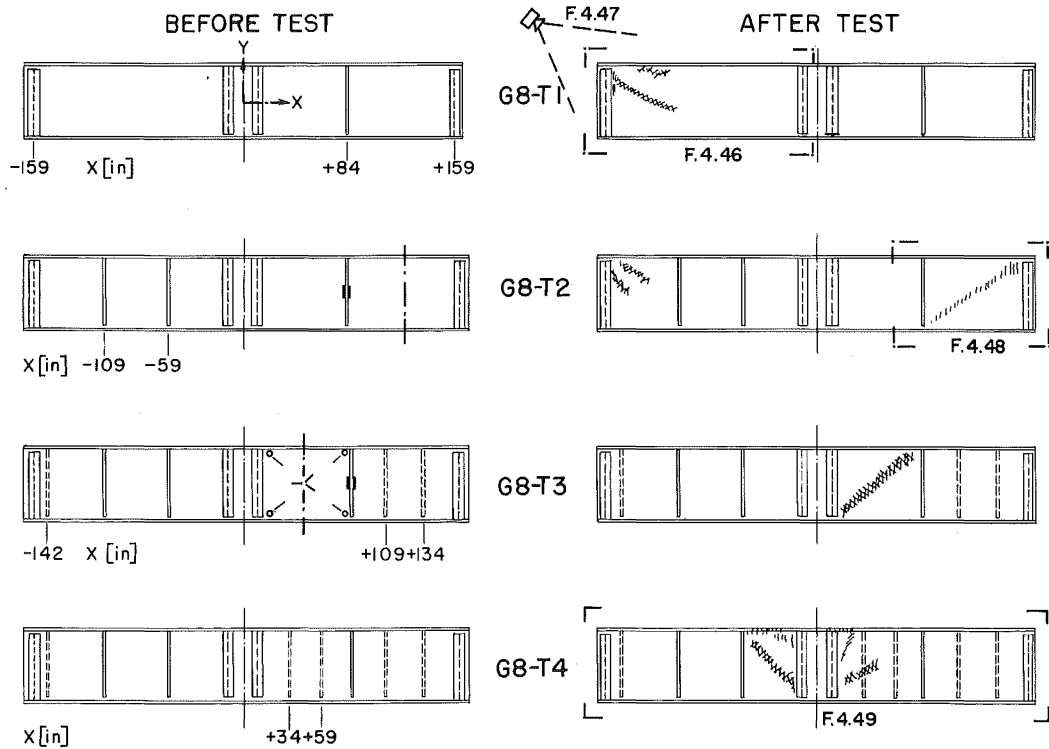


Fig. 4.41 Girder G8 Before and After Tests.

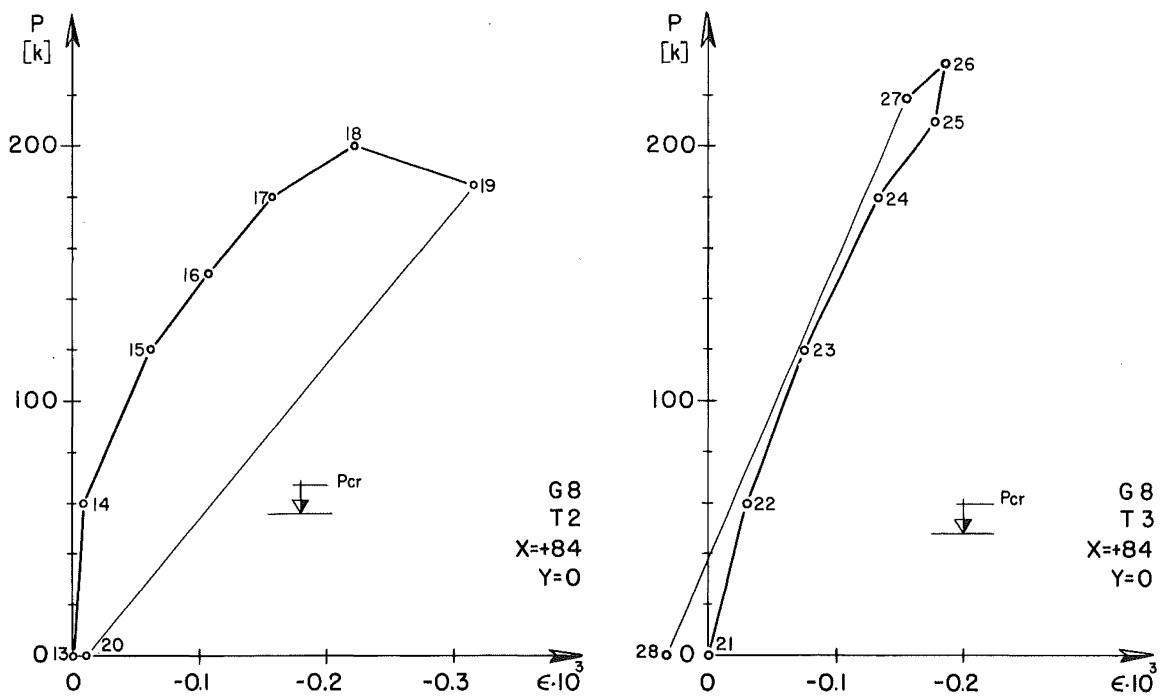


Fig. 4.42 Principal Stresses at Panel Center, Girder G8

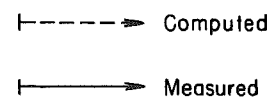
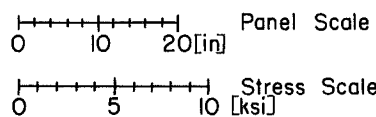
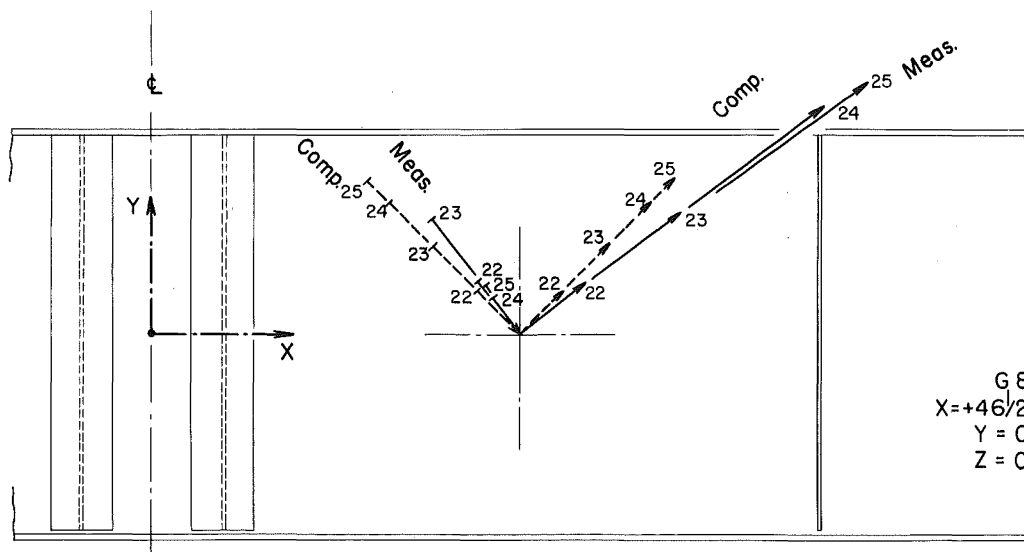


Fig. 4.43 Axial Strain in a Transverse Stiffener, Girder G8

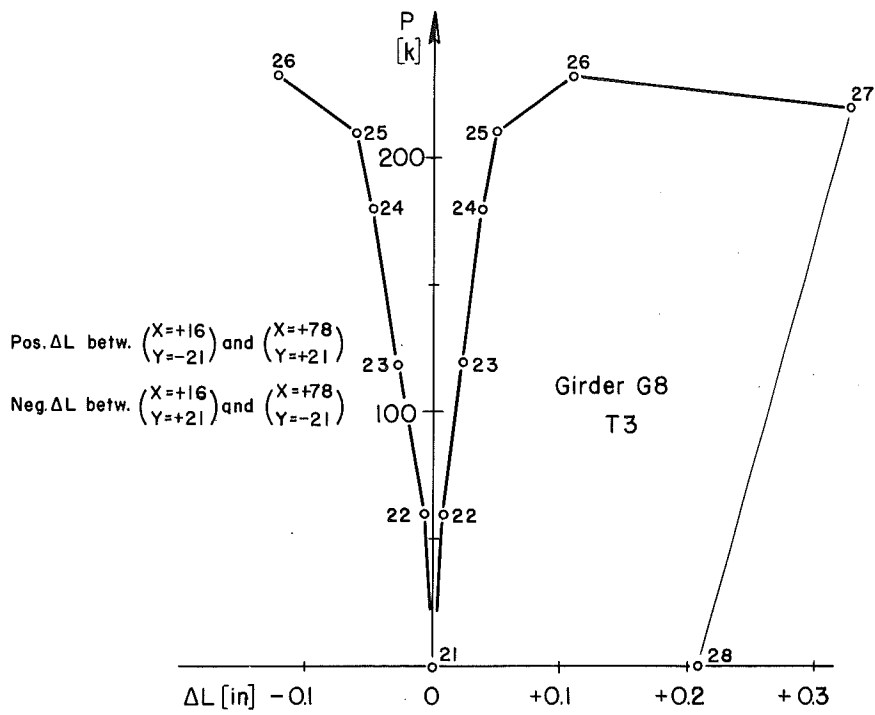


Fig. 4.44 Displacements in the Direction of Panel Diagonals, Girder G8

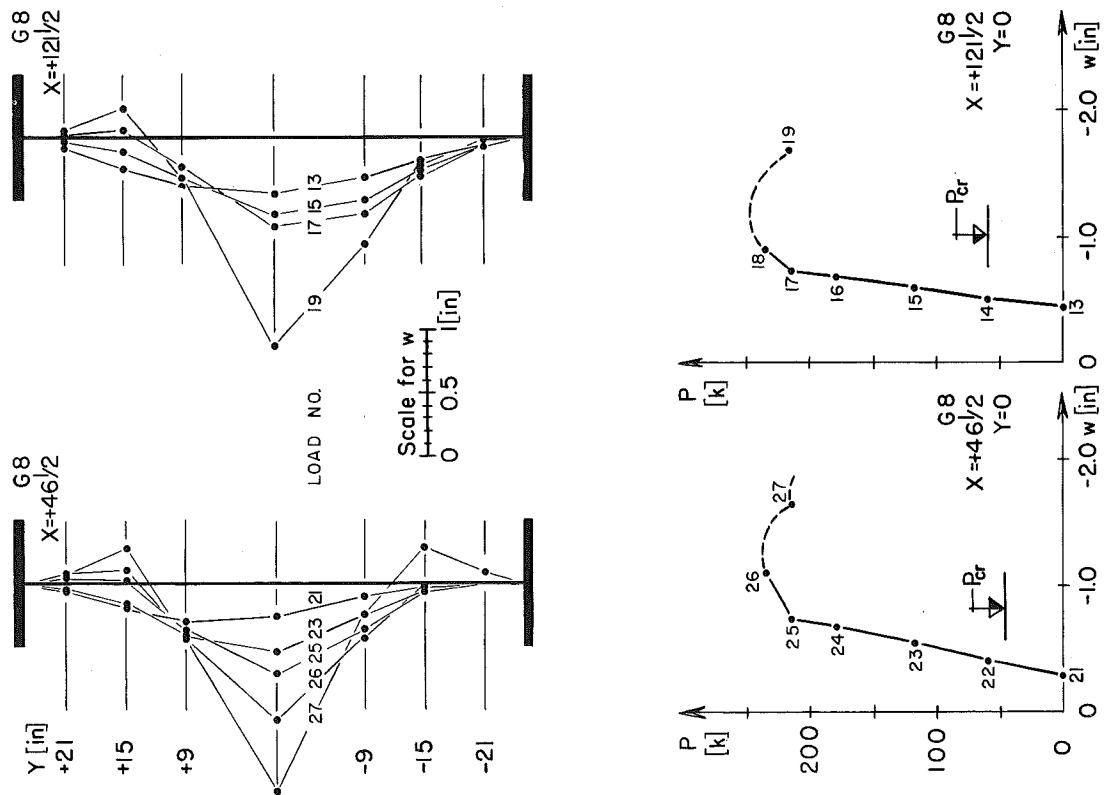


Fig. 4.45 Web Deflections, Girder G8

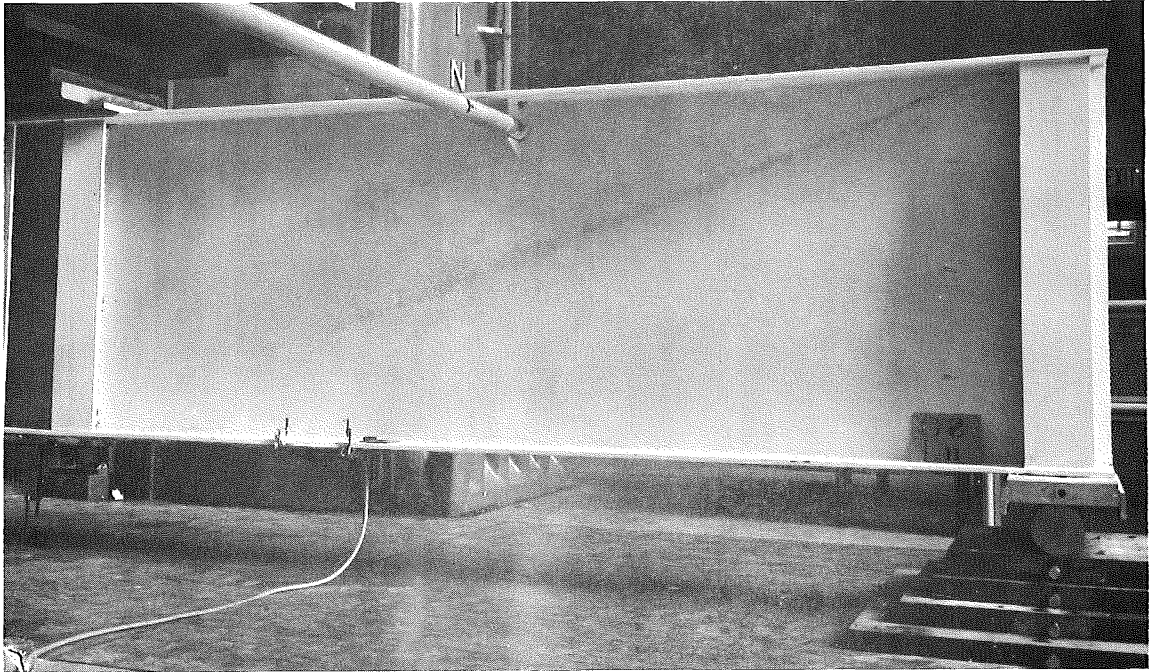


Fig. 4.46 Appearance of Girder G8 at Load No. 11, Far Side

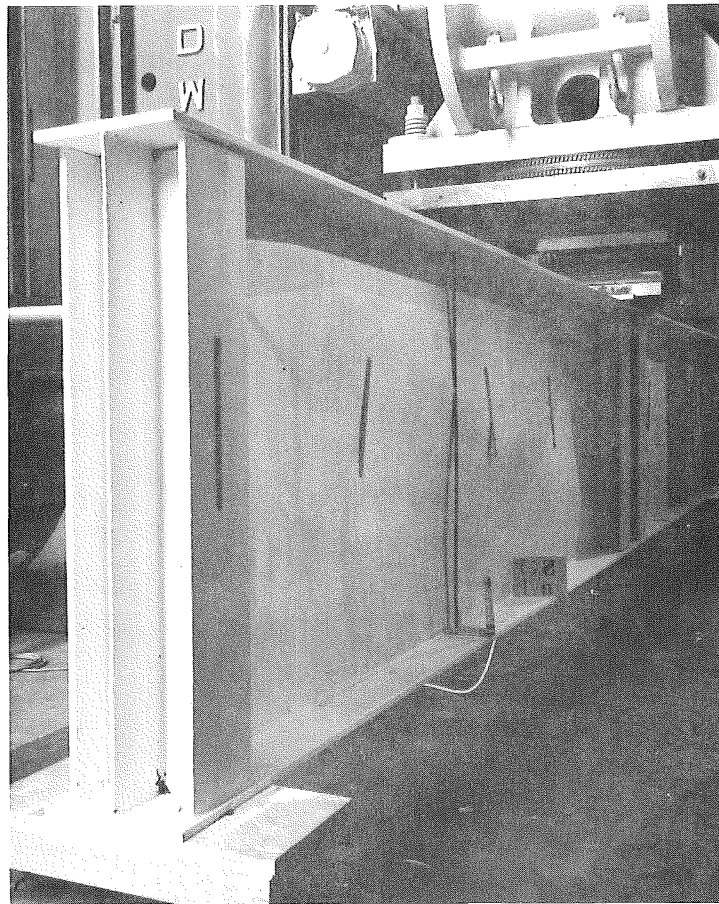


Fig. 4.47 Appearance of Girder G8 at Load No. 11, Near Side

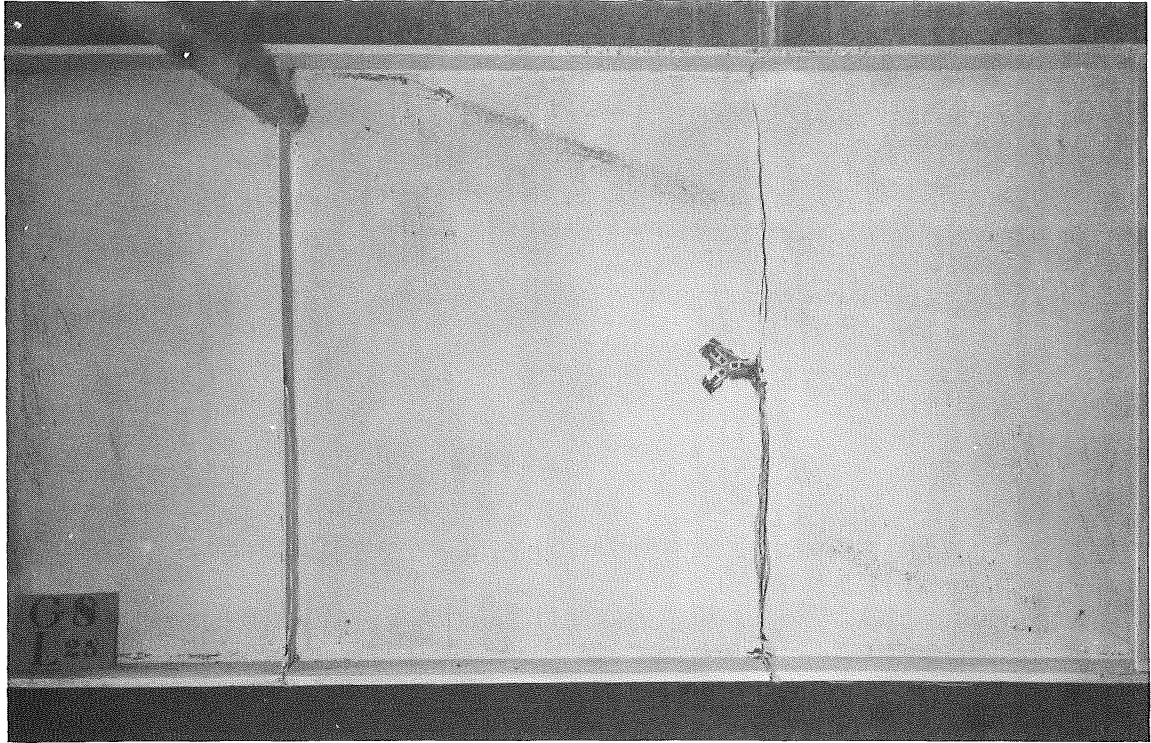


Fig. 4.48 Failure of Girder G8 in Test T3

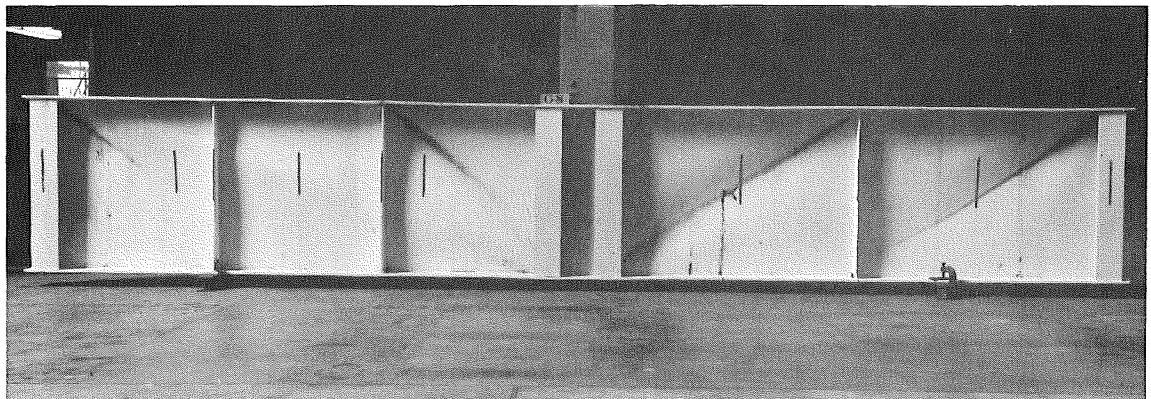


Fig. 4.49 Girder G8 After Testing

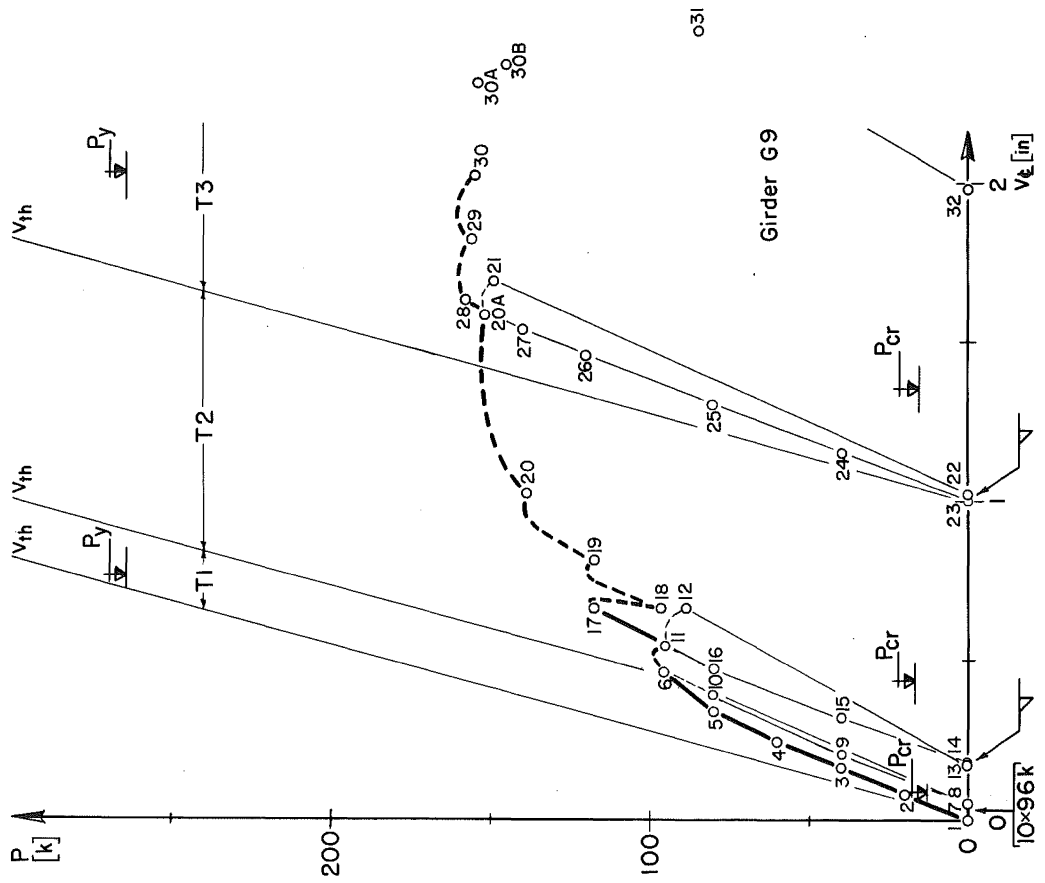


Fig. 4.50 Load-Deflection Curve, Girder G9

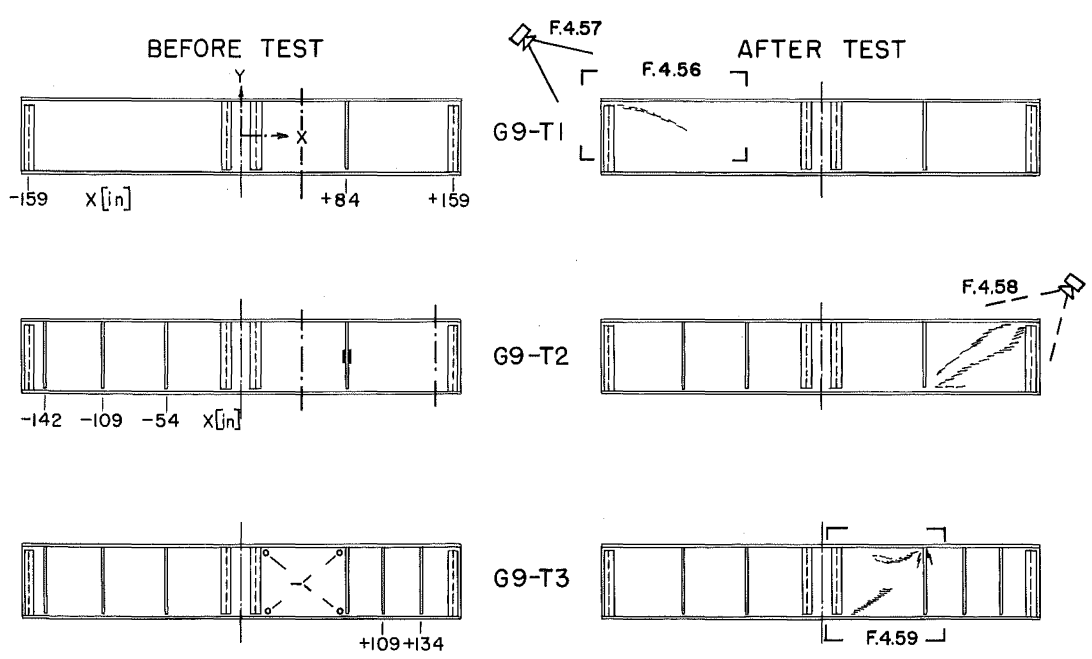


Fig. 4.51 Girder G9 Before and After Tests

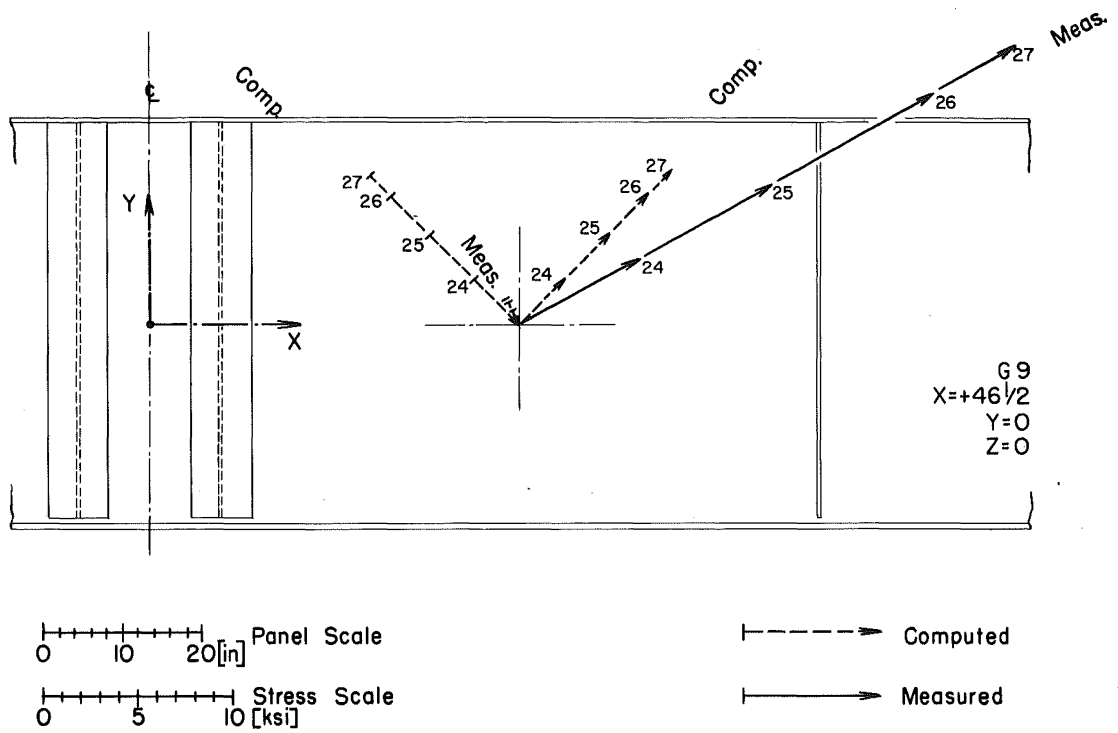


Fig. 4.52 Principal Stresses at Panel Center, Girder G9

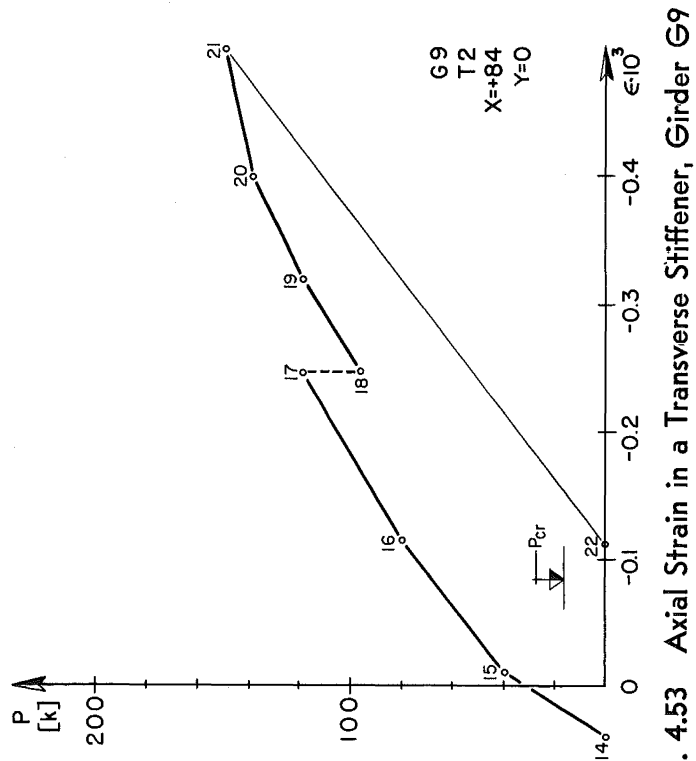


Fig. 4.53 Axial Strain in a Transverse Stiffener, Girder G9

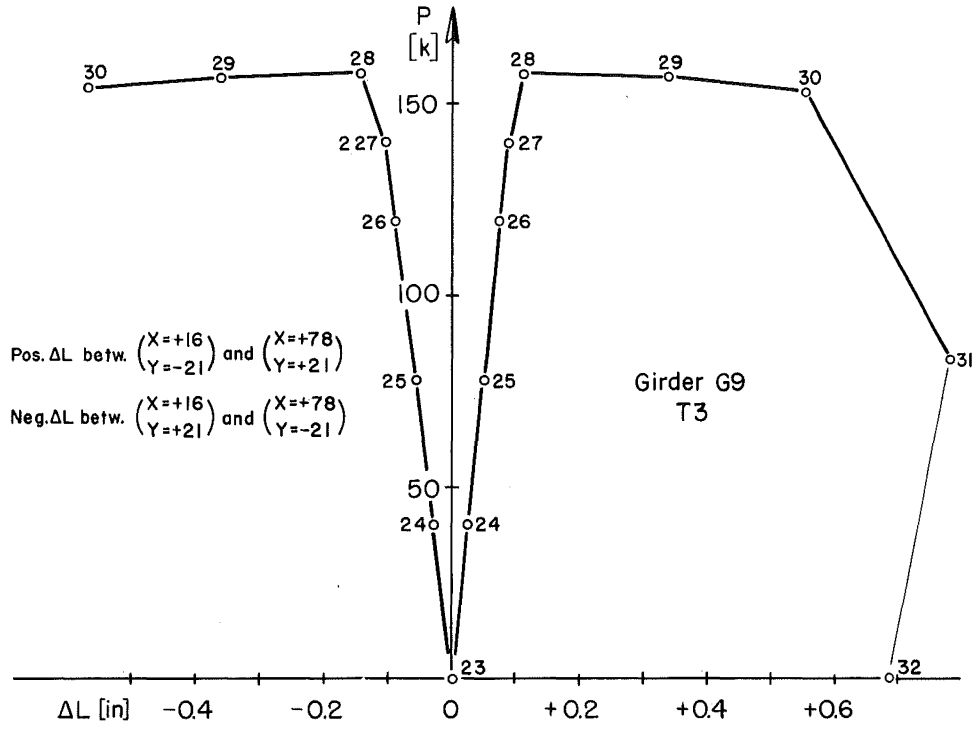


Fig. 4.54 Displacements in the Direction of Panel Diagonals, Girder G9

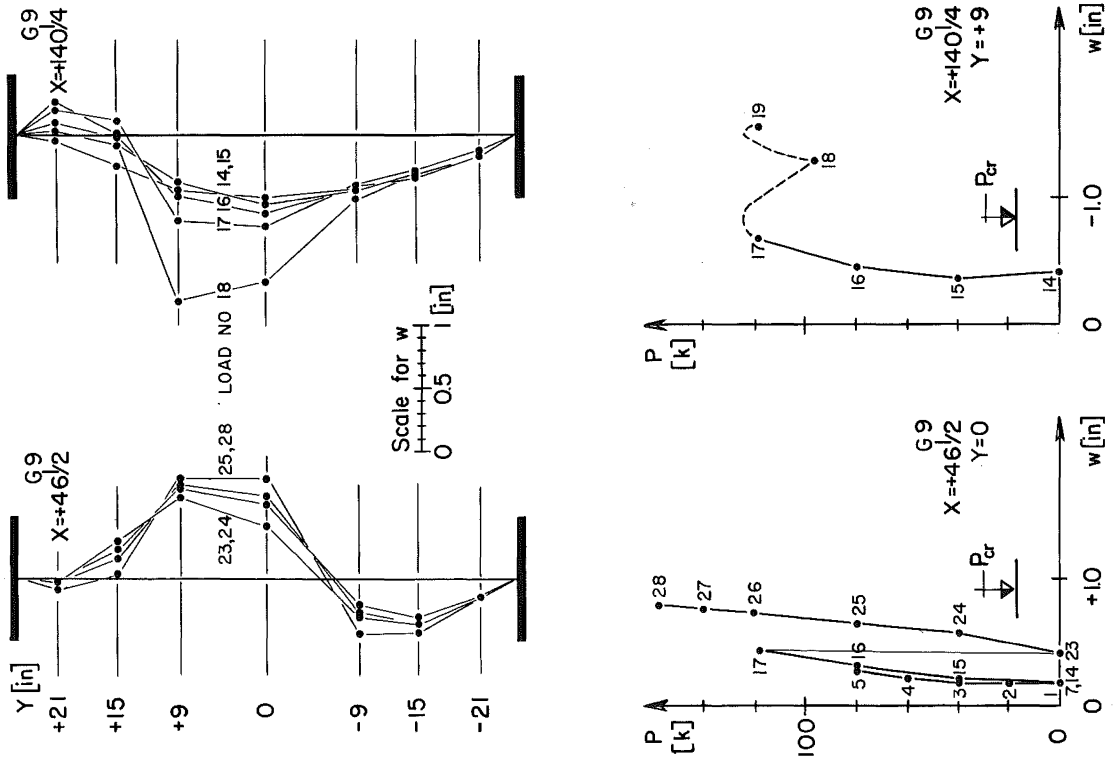


Fig. 4.55 Web Deflections, Girder G9

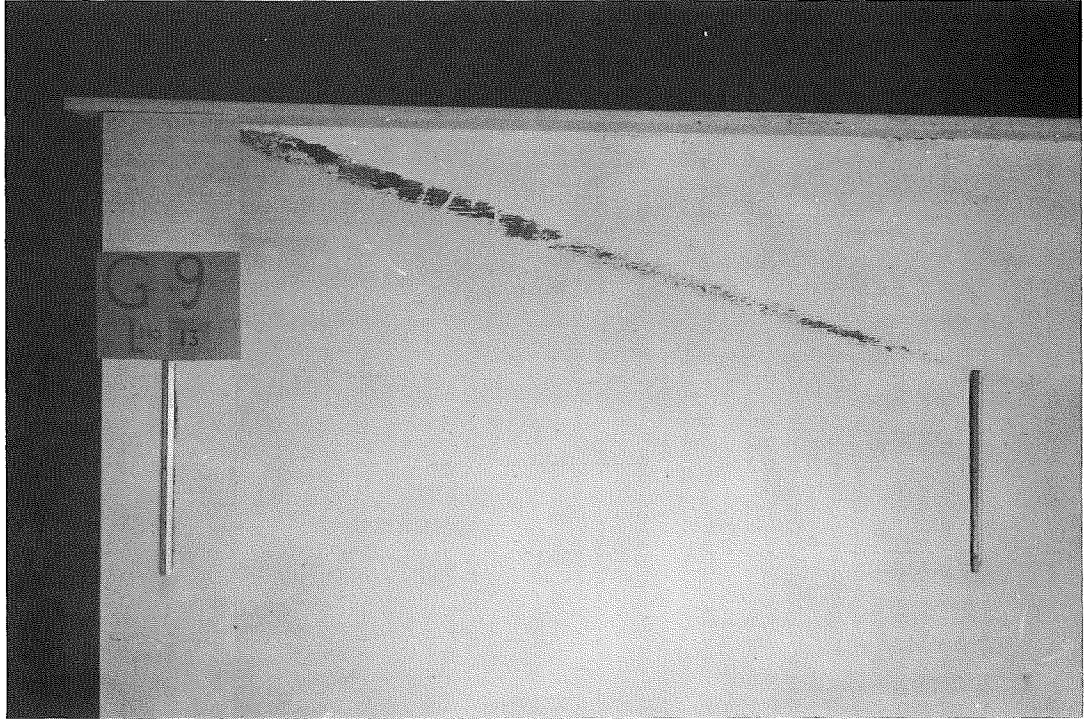


Fig. 4.56 Failure of Girder G9 in Test T1

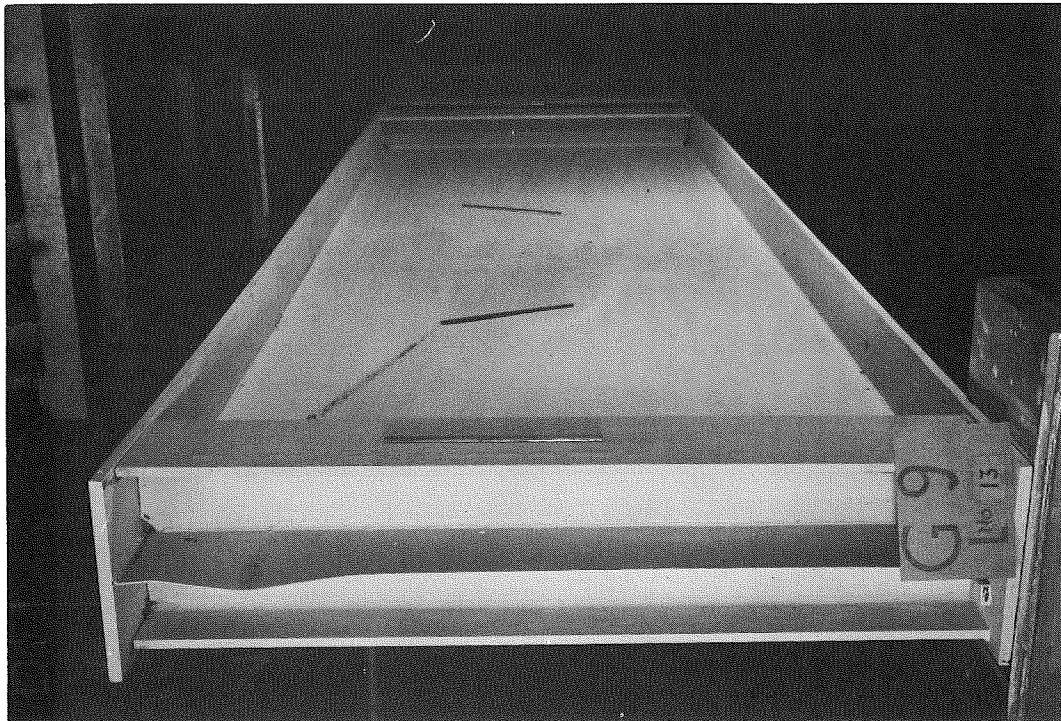


Fig. 4.57 Appearance of Girder End, Girder G9, Test T1

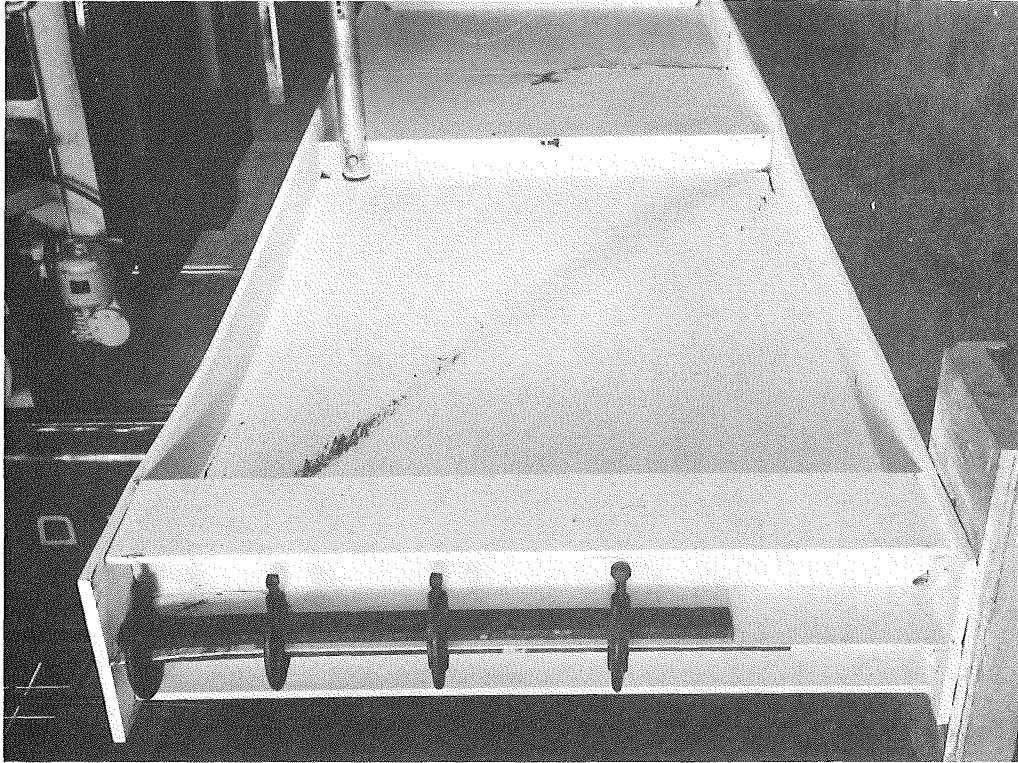


Fig. 4.58 Reinforcement After Premature End Panel Failure, Girder G9

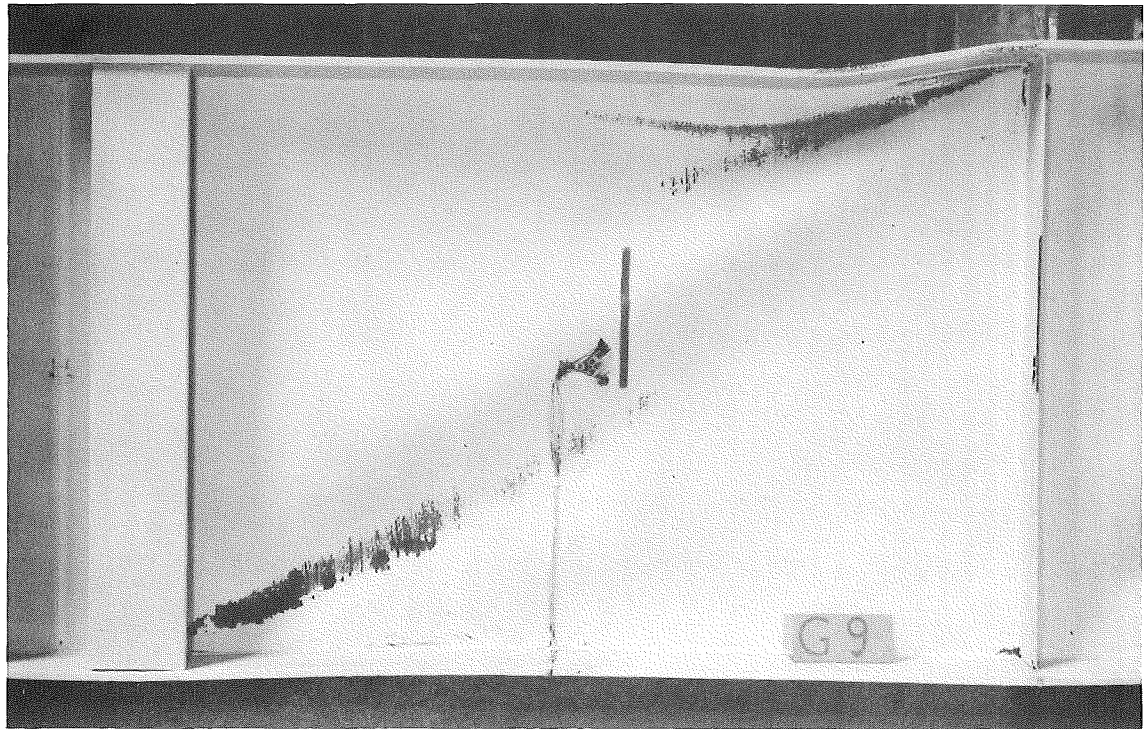


Fig. 4.59 Failure of Girder G9 in Test T3